

---

# A SURROGATE LAGRANGIAN RELAXATION-BASED MODEL COMPRESSION FOR DEEP NEURAL NETWORKS

---

A PREPRINT

Deniz Gurevin<sup>1</sup>, Shanglin Zhou<sup>2</sup>, Lynn Pepin<sup>2</sup>, Bingbing Li<sup>2</sup>, Mikhail Bragin<sup>1</sup>, Caiwen Ding<sup>2</sup>, Fei Miao<sup>2</sup>

<sup>1</sup> Department of Electrical and Computer Engineering, University of Connecticut, USA

<sup>2</sup> Department of Computer Science and Engineering, University of Connecticut, USA

{deniz.gurevin, shanglin.zhou, lynn.pepin, bingbing.li, mikhail.bragin, caiwen.ding, fei.miao}@uconn.edu

June 2, 2021

## ABSTRACT

Network pruning is a widely used technique to reduce computation cost and model size for deep neural networks. However, the typical three-stage pipeline, i.e., training, pruning and retraining (fine-tuning) significantly increases the overall training trails. For instance, the retraining process could take up to 80 epochs for ResNet-18 on ImageNet, that is 70% of the original model training trails. In this paper, we develop a systematic weight-pruning optimization approach based on Surrogate Lagrangian relaxation (SLR), which is tailored to overcome difficulties caused by the discrete nature of the weight-pruning problem while ensuring fast convergence.

We decompose the weight-pruning problem into subproblems, which are coordinated by updating Lagrangian multipliers. Convergence is then accelerated by using quadratic penalty terms.

We evaluate the proposed method on image classification tasks, i.e., ResNet-18 and ResNet-50 using ImageNet, and ResNet-18, ResNet-50 and VGG-16 using CIFAR-10, as well as object detection tasks, i.e., YOLOv3 and YOLOv3-tiny using COCO 2014, PointPillars using KITTI 2017, and Ultra-Fast-Lane-Detection using TuSimple lane detection dataset. Numerical testing results demonstrate that with the adoption of the Surrogate Lagrangian Relaxation method, our SLR-based weight-pruning optimization approach achieves a high model accuracy even at the hard-pruning stage without retraining for many epochs, such as on PointPillars object detection model on KITTI dataset where we achieve  $9.44\times$  compression rate by only retraining for 3 epochs with less than 1% accuracy loss. As the compression rate increases, SLR starts to perform better than ADMM and the accuracy gap between them increases. SLR achieves 15.2% better accuracy than ADMM on PointPillars after pruning under  $9.49\times$  compression. Given a limited budget of retraining epochs, our approach quickly recovers the model accuracy.

## 1 Introduction

Deep neural network (DNN) based statistical models are increasingly taxing of computational and storage resources. This is especially a problem for embedded or IoT devices [1, 2, 3]. These costs are related to the model size (i.e. the number of parameters in a model). By reducing model size, one reduces both computation and storage costs of evaluating a model. Various techniques exist in this area, e.g. weight pruning, sparsity regularization, quantization, clustering, aiming to reduce model size without harming the performance of the model. These techniques are collectively known as *model compression* [3, 4, 5, 6, 7, 8, 9, 10, 3, 4, 5, 6, 7, 8, 9, 10, 11, 12, 13, 3, 14, 15].

This series of works leverage the observation that training a compact model from scratch is much harder (with less accuracy) than retraining a pruned model [16, 17, 18]. Therefore, a typical three-stage pipeline, i.e., training (large model), pruning and retraining (fine-tuning) is required. The pruning process is to set the redundant weights to zero and keep the important weights to best preserve the accuracy. The retraining process is necessary since the model

accuracy dramatically drops after hard-pruning. However, this three-stage weight pruning technique significantly increases the overall training trails. For example, although the state-of-the-art Alternate Direction Method of Multipliers (ADMM)-based DNN model compression [19] achieves very high compression rate while maintaining the prediction accuracy on many DNN architectures, the retraining process takes a long time, e.g., 80 epochs for ResNet-18 on ImageNet, that is 70% of the original model training trails.

Given the pros and cons of current weight pruning-method, this paper aims at: **Is there an optimization method on weight pruning that can achieve a high model accuracy even at the hard-pruning stage and can reduce retraining trails significantly? Given a limited budget of retraining epochs, is there an optimization method that can quickly recover the model accuracy (much faster than the state-of-the-arts, e.g, ADMM)?**

The major difficulty on the path to answer these questions is the discrete nature of the model compression problems caused by "cardinality" constraints, which ensure that a certain proportion of weights is pruned.

In this paper, to address this difficulty, we develop a systematic weight-pruning optimization approach based on recent Surrogate Lagrangian relaxation (SLR) [20], which overcame all major convergence difficulties of standard Lagrangian relaxation. After decomposing the weight-pruning problem into subproblems, their solutions are coordinated by updating Lagrangian multipliers. With novel stepsizing formula, convergence of the method has been proved as long as subproblem solutions satisfy the simple "surrogate" optimality condition [20]. Convergence of the method is further accelerated by using quadratic penalties. The method thus possesses nice convergence properties inherited from fast accelerated reduction of constraint violation owing to quadratic penalties and from the guaranteed convergence following the framework of Surrogate Lagrangian Relaxation. Therefore, Lagrangian multipliers within SLR approach their optimal values much faster as compared to those within other methods, e.g., ADMM. As a result, model parameters obtained by SLR during the training phase are much closer to their optimal values as compared to those obtained by other state-of-the-art methods, e.g, ADMM. Therefore, weight pruning achieves higher model accuracy even at the hard-pruning stage as compared to ADMM. Moreover, given limited budgets of retraining epochs, the model accuracy within the SLR method is higher.

We summarize our contributions as:

- Novel SLR-based approach tailored to overcome difficulties caused by the discrete nature of the weight-pruning problem while ensuring fast convergence.
- Our SLR-based weight-pruning optimization approach achieves a high model accuracy even at the hard-pruning stage and given a limited budget of retraining epochs, it quickly recovers the model accuracy.
- As the compression rate increases, SLR starts to perform better than ADMM and the accuracy gap between them increases.

## 2 Related Works

### 2.1 Model Compression

Considering the increasing computation and weight storage of Deep Neural Networks(DNNs), model compression becomes more and more essential when we implement high efficient deep learning applications in real world. There are two common compression techniques, weight pruning and weight quantization. Since lots of researchers have investigated that some portion of weights in neural networks are redundant, weight pruning is proposed to remove these less important coefficient values and it achieves model compression with similar performance compared to uncompressed one. The weight quantization is another way to reduce the weight storage by reducing the representative weight bits.

In Han's early work [21], it proposed a iterative irregular weight pruning method that most reduction is achieved in fully-connected layers, and the reduction achieved in convolutional layers can hardly achieve any acceleration in GPUs. For weight storage, it reduces  $9\times$  the number of parameters in AlexNet and  $13\times$  in VGGNet-16.

To overcome the limitation in irregular weight pruning, structured weight pruning methods were proposed by [11]. It investigated structured sparsity at the levels of filters, channels, and filter shapes. However, the overall compression rate in structured pruning is limited compared to the unstructured pruning. In AlexNet without accuracy degradation, the average weight pruning rate on convolutional layers is only  $1.4\times$ . The recent work [22] achieved  $2\times$  channel pruning with 1% accuracy degradation on VGGNet-16.

In our work, we will focus on weight pruning method to achieve high compression rate.

## 2.2 Alternating Direction Method of Multipliers

The ADMM is an optimization algorithm that breaks optimization problems into smaller subproblems, each of which is then solved iteratively and more easily. The earliest study of ADMM can be traced back to 1970s, and a variety of statistical and machine learning problems which can be efficiently solved by using ADMM were discussed [23]. Recently, weight pruning research works achieved high compression rate and avoided significant accuracy loss by integrating the powerful ADMM [19, 24, 25]. The successful applications with ADMM outperform prior approaches by applying dynamic penalty on all targeted weights. The algorithm is applicable to different schemes of nonstructured pruning and structured pruning.

Zhang *et al.* [19] was the first work implementing an ADMM based framework on DNN weight pruning, achieving  $21 \times$  irregular weight pruning with almost no accuracy loss in AlexNet. A pattern-based weight pruning was proposed with high efficiency especially designed and optimized for mobile devices [24], it explored a fine-grained sparsity to maximize the utilization of limited resource devices. Li *et al.* [25] improved previous ADMM based structured weight pruning framework by adopting soft constraint-based formulation to achieve higher compression rate and tune fewer hyperparameters.

## 3 Systematic Weight Pruning Framework using SLR

Consider a DNN with layers indexed by  $i \in 1..N$ , where the weights and biases of a given layer  $i$  is denoted by  $\mathbf{W}_i$  and  $\mathbf{b}_i$ , respectively. The loss function is denoted by  $f(\{\mathbf{W}_i\}_{i=1}^N, \{\mathbf{b}_i\}_{i=1}^N)$ . Our objective is to prune the weights of the DNN, therefore we minimize the loss function subject to constraints on the cardinality of weights in each layer. More specifically, our training process solves a recent decomposition and coordination ‘‘Surrogate Lagrangian Relaxation’’ (SLR) method [20] which will be used for DNN training.

The weight pruning optimization problem can be written as

$$\underset{\{\mathbf{W}_n\}, \{\mathbf{b}_n\}}{\text{minimize}} \quad f(\{\mathbf{W}_n\}, \{\mathbf{b}_n\}), \quad (1)$$

$$\text{subject to} \quad \mathbf{W}_n \in \mathbf{S}_n, \quad n = 1, \dots, N, \quad (2)$$

where  $\mathbf{S}_n = \{\mathbf{W}_n \mid \text{card}(\mathbf{W}_n) \leq l_n\}$ ,  $n = 1, \dots, N$ . The resulting problem belongs to the class of nonlinear discrete optimization problems: non-linearity comes from the non-linearity of the objective function and discrete (binary) variables are implicitly captured by the ‘‘cardinality’’ constraints (2) within sets  $\mathbf{S}_1, \dots, \mathbf{S}_N$ .

The problem (1)-(2) can be equivalently rewritten in an unconstrained form as

$$\underset{\{\mathbf{W}_n\}, \{\mathbf{b}_n\}}{\text{minimize}} \quad f(\{\mathbf{W}_n\}, \{\mathbf{b}_n\}) + \sum_{n=1}^N g_n(\mathbf{W}_n), \quad (3)$$

where  $g_n(\cdot)$  is the indicator function of  $\mathbf{S}_n$ , i.e.,

$$g_n(\mathbf{W}_n) = \begin{cases} 0 & \text{if } \text{card}(\mathbf{W}_n) \leq l_n, \quad n = 1, \dots, N, \\ +\infty & \text{otherwise.} \end{cases}$$

In Problem (3), the first term represents the DNN’s nonlinear smooth loss function and the second term represents the non-differentiable ‘‘cardinality’’ penalty term [19]. The problem cannot be solved by analytically or stochastic gradient descent in its entirety. To enable the decomposition, duplicate variables are introduced and the problem is equivalently rewritten as follows

$$\underset{\{\mathbf{W}_n\}, \{\mathbf{b}_n\}}{\text{minimize}} \quad f(\{\mathbf{W}_n\}, \{\mathbf{b}_n\}) + \sum_{n=1}^N g_n(\mathbf{Z}_n), \quad (4)$$

$$\text{subject to} \quad \mathbf{W}_n = \mathbf{Z}_n, \quad n = 1, \dots, N. \quad (5)$$

In the following, to lay out the foundation for the dual approaches that make use of quadratic penalty terms, the Augmented Lagrangian Relaxation will be presented and its difficulties will be highlighted. Then, the Surrogate Lagrangian Relaxation approach will be developed to solve the problem (4)-(5).

**Augmented Lagrangian Relaxation.** To solve the problem (4)-(5), constraints (5) are first relaxed by introducing Lagrangian multipliers and their violations are penalized by using quadratic penalties. The resulting augmented

Lagrangian function [26, 19] of the above optimization problem is this given by

$$\begin{aligned}
L_\rho(\{\mathbf{W}_n\}, \{\mathbf{b}_n\}, \{\mathbf{Z}_n\}, \{\Lambda_n\}) &= f(\{\mathbf{W}_n\}, \{\mathbf{b}_n\}) + \sum_{n=1}^N g_n(\mathbf{Z}_n) \\
&+ \sum_{n=1}^N \text{tr}[\Lambda_n^T(\mathbf{W}_n - \mathbf{Z}_n)] + \sum_{n=1}^N \frac{\rho}{2} \|\mathbf{W}_n - \mathbf{Z}_n\|_F^2,
\end{aligned} \tag{6}$$

where  $\Lambda_n$  is a matrix of Lagrangian multipliers (dual variables) corresponding to constraints  $\mathbf{W}_n = \mathbf{Z}_n$ , and has the same dimension as  $\mathbf{W}_n$ . The positive scalar  $\rho$  is the penalty coefficient,  $\text{tr}(\cdot)$  denotes the trace, and  $\|\cdot\|_F^2$  denotes the Frobenius norm.

The Augmented Lagrangian Relaxation is the dual approach, whereby the following relaxed problem is solved at the low level first to obtain the dual value as:

$$q_\rho(\{\Lambda_n\}) = \min_{\{\mathbf{W}_n\}, \{\mathbf{b}_n\}, \{\mathbf{Z}_n\}} L_\rho(\{\mathbf{W}_n\}, \{\mathbf{b}_n\}, \{\mathbf{Z}_n\}, \{\Lambda_n\}). \tag{7}$$

Generally, after (7) is solved for given values of multipliers  $\Lambda_n^k$ , multipliers are updated at the high level based on the levels of constraint violations  $\mathbf{W}_n^k - \mathbf{Z}_n^k$  (also referred to as ‘‘subgradient directions’’) until convergence to the optimal multipliers  $\{\Lambda_n^*\}$  which maximize the dual function  $q_\rho(\{\Lambda_n\})$  given in (7). From the practical implementation prospective, however, there are several difficulties: 1) The relaxed problem (7) can still not be solved in its entirety by any existing method; 2) As discussed in Introduction, because of the discrete nature of the original problem (1)-(2) caused by ‘‘cardinality’’ constraints, the corresponding dual function is non-smooth. The non-smoothness of the dual function  $q_\rho(\{\Lambda_n\})$ , in turn, leads to other difficulties such as 2.1) zigzagging of multipliers, 2.2) the need to know the optimal dual value  $q_\rho(\{\Lambda_n^*\})$  for convergence.

In the following, motivated by decomposibility enabled by Surrogate Lagrangian Relaxation (SLR) [20, 27], which overcame all major difficulties of standard Lagrangian Relaxation, with much alleviated zigzagging and guaranteed convergence, the relaxed problem will be decomposed into two manageable subproblems, and the subproblems will then be efficiently coordinated by Lagrangian multipliers.

**Decomposition though SLR.** The first difficulty mentioned above will be resolved by decomposing the relaxed problem (7) into the the following subproblems:

**Step 1: Solve ‘‘Loss Function’’ Subproblem for  $\mathbf{W}_n$  and  $\mathbf{b}_n$  using Stochastic Gradient Decent.** At iteration  $k$ , for a given values of multipliers  $\Lambda_n^k$ , the first ‘‘loss function’’ subproblem is to minimize the Lagrangian function with respect to weights and biases, while keeping  $\mathbf{Z}_n$  at previously obtained values  $\mathbf{Z}_n^{k-1}$  as

$$\min_{\{\mathbf{W}_n\}, \{\mathbf{b}_n\}} L_\rho(\{\mathbf{W}_n\}, \{\mathbf{b}_n\}, \{\mathbf{Z}_n^{k-1}\}, \{\Lambda_n\}). \tag{8}$$

Since the regularizer is a differentiable quadratic norm, and the loss function of the DNN is differentiable, the subproblem can be solved by stochastic gradient descent. More specifically, the gradients of objective function within (8) with respect to  $\mathbf{W}_n$  and  $\mathbf{b}_n$  are given by

$$\frac{\partial L_\rho(\{\mathbf{W}_n\}, \{\mathbf{b}_n\}, \{\mathbf{Z}_n^{k-1}\}, \{\Lambda_n^k\})}{\partial \mathbf{W}_n} = \frac{\partial f(\{\mathbf{W}_n\}, \{\mathbf{b}_n\})}{\partial \mathbf{W}_n} + \Lambda_n^k + \rho(\mathbf{W}_n - \mathbf{Z}_n^{k-1}),$$

$$\frac{\partial L_\rho(\{\mathbf{W}_n\}, \{\mathbf{b}_n\}, \{\mathbf{Z}_n^{k-1}\}, \{\Lambda_n^k\})}{\partial \mathbf{b}_n} = \frac{\partial f(\{\mathbf{W}_n\}, \{\mathbf{b}_n\})}{\partial \mathbf{b}_n}.$$

**Step 2: Solve ‘‘Cardinality’’ Subproblem for  $\mathbf{Z}_n$  through Pruning by using Projections onto Discrete Subspace.** The second ‘‘cardinality’’ subproblem is solved with respect to  $\mathbf{Z}_n$  while fixing other variables at values  $\mathbf{W}_n^k$  and  $\mathbf{b}_n^k$  as

$$\min_{\{\mathbf{Z}_n\}} L_\rho(\{\mathbf{W}_n^k\}, \{\mathbf{b}_n^k\}, \{\mathbf{Z}_n\}, \{\Lambda_n^k\}). \tag{9}$$

Since  $g_n(\cdot)$  is the indicator function of the set  $\mathbf{S}_n$ , the globally optimal solution of this problem can be explicitly derived as [26]:

$$\mathbf{Z}_n^k = \Pi_{\mathbf{S}_n}(\mathbf{W}_n^k + \frac{\Lambda_n^k}{\rho}), \quad (10)$$

where  $\Pi_{\mathbf{S}_n}(\cdot)$  denote the Euclidean projections onto sets  $\mathbf{S}_n$ .

While the relaxed problem is decomposed into 1) the ‘‘loss function’’ subproblem (8), which can be solved by stochastic gradient descent, and 2) the ‘‘cardinality’’ subproblem (9), which can be solved analytically, in practical implementation, the exact optimality of solutions  $\{\mathbf{W}_n^k\}, \{\mathbf{b}_n^k\}$  to the ‘‘loss function’’ subproblem (8) cannot generally be proved. As a result, the multiplier-updating direction  $\mathbf{W}_n^k - \mathbf{Z}_n^k$ , unlike subgradient direction, may not form acute angles with directions toward the optimal multipliers, which may result in divergence. These coordination issues will be resolved by the ‘‘surrogate’’ optimality condition as will be discussed next.

**Step 3: Update  $\Lambda_n$  Based on Smooth ‘‘Surrogate’’ Directions: Efficient Coordination through Surrogate Lagrangian Relaxation.** While the optimality of the solutions to the ‘‘loss function’’ subproblem (8) cannot be guaranteed after every epoch, within the ‘‘surrogate subgradient method’’ [28], the satisfaction of a much ‘‘softer’’ requirement - the ‘‘surrogate optimality condition,’’ is sufficient in order to proceed with the update of multipliers. In terms of the augmented Lagrangian function (6), the surrogate optimality condition is written as follows:

$$L_\rho(\{\mathbf{W}_n^k\}, \{\mathbf{b}_n^k\}, \{\mathbf{Z}_n^k\}, \{\Lambda_n^k\}) < L_\rho(\{\mathbf{W}_n^{k-1}\}, \{\mathbf{b}_n^{k-1}\}, \{\mathbf{Z}_n^{k-1}\}, \{\Lambda_n^k\}) \quad (11)$$

Once (11) is satisfied,<sup>1</sup> multipliers are updated as

$$\Lambda_n^{k+1} := \Lambda_n^k + s^k(\mathbf{W}_n^k - \mathbf{Z}_n^k), \quad (12)$$

where stepsizes are set as:

$$s^k = \alpha^k \frac{s^k \|\mathbf{W}_n^{k-1} - \mathbf{Z}_n^{k-1}\|}{\|\mathbf{W}_n^k - \mathbf{Z}_n^k\|}, \quad (13)$$

and the stepsize-setting parameters are:

$$\alpha^k = 1 - \frac{1}{M \times k^{(1-\frac{1}{k^r})}}, M > 1, 0 < r < 1. \quad (14)$$

Here  $M$  and  $r$  are hyper-parameters.

As proved in [20], if the surrogate optimality condition (11) is satisfied ‘‘periodically’’ and ‘‘infinitely’’ often, and stepsizes are set up according to (13)-(14), multipliers converge to the optimum. In Section 4, it will be empirically verified that condition (11) is satisfied throughout the entire iterative process, periodically, and frequently.

The algorithm of the new method is presented below:

---

**Algorithm 1:** Surrogate Lagrangian Relaxation

---

Initialize  $\{\mathbf{W}_n^0\}, \{\mathbf{b}_n^0\}, \{\mathbf{Z}_n^0\}, \{\Lambda_n^0\}$  and  $s^0$   
**while** *Stopping criteria are not satisfied* **do**  
    **1** solve subproblems (8) and (9) and update multipliers per (12) ;  
    **if** *surrogate optimality condition (11) is satisfied* **then**  
        keep  $\{\mathbf{W}_n^k\}, \{\mathbf{b}_n^k\}, \{\mathbf{Z}_n^k\}, \{\Lambda_n^k\}$ , goto 1;  
    **else**  
        keep  $\{\mathbf{W}_n^k\}, \{\mathbf{b}_n^k\}, \{\mathbf{Z}_n^k\}$ , discard  $\{\Lambda_n^k\}$ , goto 1  
    **end**  
**end**

---

The norm of the constraint violation, number of steps or CPU time can be used as stopping criteria for the algorithm above.

---

<sup>1</sup>If condition (11) is not satisfied, the subproblems (8) and (9) are solved again by using the latest available values for  $\{\mathbf{W}_n\}, \{\mathbf{b}_n\}$  and  $\{\mathbf{Z}_n\}$ .

Table 1: Comparison of SLR and ADMM on CIFAR-10 and ImageNet datasets. ImageNet results are based on Top-5 accuracy.

Dataset	Architecture	Model Accuracy (%)	Optimization	After Training (%)	After Hardpruning (%)	After Retraining (%)	Compression Rate
CIFAR-10	ResNet-18	93.33	ADMM	75.45	80.25	89.73	8.71×
			SLR	88.26	88.12	90.37	
	ResNet-50	93.86	ADMM	95.93	88.74	90.97	3.4×
			SLR	89.50	92.26	92.10	
	VGG-16	93.27	ADMM	91.64	91.68	92.84	3.08×
			SLR	92.82	92.04	92.85	
ImageNet	ResNet-18	89.07	ADMM	81.37	80.69	85.23	6.5×
			SLR	83.00	83.31	85.66	
	ResNet-50	92.87	ADMM	86.82	88.46	89.52	3.89×
			SLR	87.86	88.82	89.95	

Table 2: ADMM and SLR training results with YOLOv3 on COCO benchmark.

Model	Epochs	Original mAP	Optimization	After Training	After Hardpruning	Compression Rate
YOLOv3-tiny	15	37.1	ADMM	33.9	33.2	1.19×
			SLR	34.6	<b>34.6</b>	
	20	37.1	ADMM	31.7	30.6	2×
			SLR	33.6	<b>33.5</b>	
	40	37.1	ADMM	33.9	33.2	3.33×
			SLR	34.6	<b>34.6</b>	
YOLOv3-SPP	30	64.4	ADMM	59.3	52.0	1.986×
			SLR	59.7	<b>54.5</b>	

## 4 Evaluation

In this section, we present our experimental results to evaluate SLR performance and compare ADMM and SLR methods. In Section 4.1, we will introduce our evaluation metrics for our experiments. In Section 4.2, we present our experimental results for image classification tasks on CIFAR-10 and ImageNet datasets. In Section 4.3, we present our experimental results for object detection tasks on COCO and KITTI object detection benchmarks, and a lane detection task on TuSimple lane detection benchmark. Finally, in Section 4.4, we discuss the ablation studies on SLR.

### 4.1 Evaluation Metrics

In order to evaluate the performance of the SLR method, we follow a framework similar to [19]. We start by pruning the pretrained models through SLR training using irregular pruning. After SLR training, we perform hard-pruning on the model, which completes the compression phase of the model based on the given sparsity configuration. Finally, the model is masked-retrained to recover the accuracy which was penalized during the pruning step. As emphasized in Section 1, if the accuracy loss after pruning is high, as a result, the model suffers from longer retraining phase. Therefore, in our experiments, we evaluate the efficiency of the method based on the accuracy of the model after hard-pruning. We compare our SLR method against ADMM by comparing the accuracy of the model after SLR and ADMM training, after hard-pruning and after masked-retraining.

### 4.2 Evaluation on Image Classification Tasks

We first introduce our experimental setup, the models and datasets we use for our image classification experiments in Section 4.2.1. In Section 4.2.2, we compare SLR and ADMM performance.

#### 4.2.1 Experimental Setup

**Environmental Settings.** All of the baseline models we use and our code in this section are implemented with PyTorch 1.6.0 and Python 3.6. We conducted our experiments on Ubuntu 18.04 and using Nvidia Quadro RTX 6000 GPU with 24 GB GPU memory. We used 1 GPU node for all CIFAR-10 experiments and used 4 GPU nodes to train our models on the ImageNet dataset.

**Models and Datasets.** We compare our SLR method against ADMM. We tested our SLR method as well as the ADMM, by using 3 DNN models (ResNet-18, ResNet-50 [29] and VGG-16 [2]) on CIFAR-10 and 2 DNN models (ResNet-18 and ResNet-50) on ImageNet ILSVRC 2012 benchmark. We use the pretrained ResNet models on ImageNet from Torchvision’s “models” subpackage. The accuracy of the pretrained baseline models we used are listed in Table 1.

**Training Settings.** In all experiments we used  $\rho = 0.1$ . In CIFAR-10 experiments, we used a learning rate of 0.01, batch size of 128 and ADAM optimizer during training. On ImageNet, we used a learning rate of  $10^{-4}$ , batch size of 256 and SGD optimizer. For a fair comparison of SLR and ADMM methods, we used the same number of training epochs and sparsity configuration for both methods in the experiments.

#### 4.2.2 Comparison of ADMM and SLR

Table 1 shows our comparison of SLR and ADMM on CIFAR-10 and ImageNet benchmark. Here, SLR parameters are set as  $M = 200$ ,  $r = 0.1$  and  $s_0 = 10^{-4}$ . We used 40 epochs for both SLR and ADMM training on the CIFAR-10 experiments. On ImageNet, we used 40 epochs on ResNet-18 and 60 epochs for ResNet-50. Finally, we report the accuracy after hard pruning and after 5 epochs of masked-retraining. According to our results, SLR outperforms ADMM method in terms of both the accuracy after hard-pruning and the accuracy after retraining. Figure 2 demonstrates the reduction of constraint violation within ADMM and SLR during the training of ResNet-18 on ImageNet benchmark. It can be seen that SLR converges faster than ADMM.

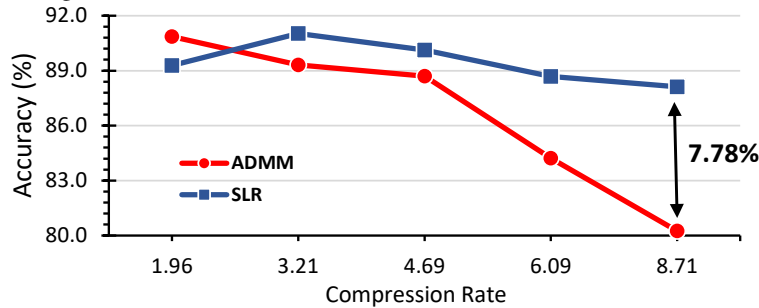


Figure 1: Accuracy of ResNet-18 (CIFAR-10) after hard-pruning with ADMM vs. SLR training for several compression rates.

Figure 1 shows the accuracy of ResNet-18 on CIFAR-10 after hard pruning for various compression rates. Here, our observation is that for a small compression rate such as  $1.96\times$ , SLR does not have a clear advantage over ADMM in terms of accuracy. However, as the compression rate increases, SLR starts to perform better than ADMM and the accuracy gap between them increases. For example, SLR can achieve  $8.71\times$  compression while ADMM can achieve  $3.21\times$  compression on ResNet18 under the same final accuracy. With  $8.71\times$  compression, SLR has 7.87% higher accuracy than ADMM. This shows that our SLR-based training method has a greater advantage over ADMM especially in higher compression rates, since it can achieve compression with less accuracy loss and consequently reduce the time required to retrain after hard-pruning.

#### 4.3 Evaluation on Object Detection Tasks

We first introduce our experimental setup and introduce the models and datasets we use for our image classification experiments in Section 4.3.1 and in Section 4.3.2, we compare SLR and ADMM performance on our object detection experiments.

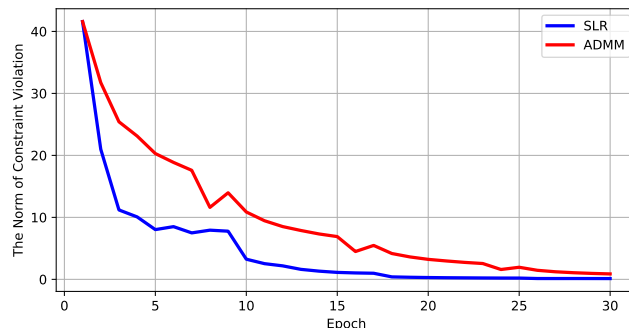
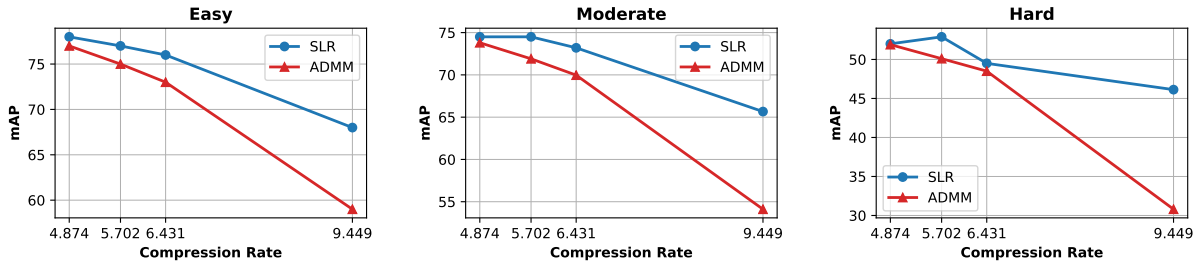


Figure 2: Convergence behavior of SLR vs. ADMM on ResNet-18 model during the training on ImageNet dataset. SLR converges faster than ADMM.

Table 3: ADMM and SLR results of PointPillars model on KITTI benchmark in different task difficulty levels and in compression rates.

Level	Original mAP	Compression	ADMM		SLR	
			After Hardpruning	After Retraining	After Hardpruning	After Retraining
Easy	80.7	4.874×	77.0	81.5	77.8	82.2
		5.702×	74.7	74.7	77.3	79.3
		6.431×	72.9	77.5	76.6	75.3
		9.449×	58.6	70.9	68.0	79.9
Moderate	78.5	4.874×	73.8	77.1	74.5	78.4
		5.702×	71.9	71.0	74.5	75.3
		6.431×	69.9	73.2	73.2	72.7
		9.449×	54.1	66.8	65.6	75.8
Hard	60.7	4.874×	51.9	51.2	52.0	56.4
		5.702×	50.1	50.2	52.9	51.3
		6.431×	48.5	47.8	49.5	50.7
		9.449×	30.8	35.6	46.1	51.4



(a) Pruning on Easy task level.

(b) Pruning on Moderate task level.

(c) Pruning on Hard task level.

Figure 3: mAP of PointPillars model after hard-pruning using different compression rates and task difficulty levels.

### 4.3.1 Experimental Setup

**Environmental Settings.** We ran our experiments on Ubuntu 18.04 and using Nvidia Quadro RTX 6000 GPU with 24 GB GPU memory. For our experiments on COCO 2014 dataset, we used Python 3.6 with Torch v1.6.0, pycocotools v2.0 packages. For our experiments on KITTI 3D object detection benchmark dataset [30] and experiments on TuSimple lane detection benchmark dataset<sup>2</sup>, we used Python 3.7 with Torch v1.6.0, and SpConv v1.2 package.

**Models and Datasets.** We used YOLOv3 and YOLOv3-tiny models [31] on COCO 2014 benchmark. We used and followed the publicly available Ultralytics repository<sup>3</sup> for YOLOv3 and its pretrained models. For 3D object detection, we used PointPillars [32] pretrained model on KITTI 2017 dataset follows OpenPCDet repository<sup>4</sup>. For lane detection experiment, we used pretrained model from Ultra-Fast-Lane-Detection [33] on TuSimple lane detection benchmark dataset.

**Training Settings.** In all experiments we used  $\rho = 0.1$ . We set SLR parameters as  $M = 200$ ,  $r = 0.1$  and  $s_0 = 10^{-4}$ . We follow the same training settings provided by the repositories we use. Finally, we use the same number of training epochs and sparsity configuration for ADMM and SLR.

**Testing Settings.** On YOLOv3 models, we calculate the COCO mAP with IoU = 0.50 with image size of 640 for testing. On 3D object detection experiments, LIDAR point cloud is used as input. The KITTI dataset is stratified into easy, moderate, and hard difficulties. mAP is calculated under each difficulty strata with IoU = 0.5. On lane detection experiments, evaluation metric is ‘‘accuracy’’, which is calculated as  $\frac{\sum_{clip} C_{clip}}{\sum_{clip} S_{clip}}$ , where  $C_{clip}$  is the number of lane points predicted correctly and  $S_{clip}$  is the total number of ground truth in each clip.

### 4.3.2 Comparison of ADMM and SLR

Our comparison of SLR and ADMM methods on COCO dataset is shown in Table 2. We have compared the two methods under 3 different compression rates for YOLOv3-tiny and tested YOLOv3-SPP pre-trained model with a compression rate of 1.98. We can see that the model pruned with SLR method has higher accuracy after hard-pruning

<sup>2</sup><https://github.com/TuSimple/tusimple-benchmark>

<sup>3</sup><https://github.com/ultralytics/yolov3>

<sup>4</sup><https://github.com/open-mmlab/OpenPCDet>

Table 4: ADMM and SLR training results on TuSimple benchmark through different compression rates.

Compression Rate	Method	(%) After Training	(%) After Hardpruning	(%) After Retraining
1.82×	ADMM	92.87	92.76	94.20
	SLR	94.76	94.63	94.83
2.54×	ADMM	93.59	93.50	94.38
	SLR	94.59	94.57	94.59
4.21×	ADMM	93.83	90.66	94.46
	SLR	94.06	92.54	94.63

in all cases. In compression rate 3.33 on YOLOv3-tiny, ADMM and SLR have similar performance due to the longer training (40 epochs). However, when trained for 20 epochs with a compression rate of 2, we observe that SLR has higher mAP since it can converge faster than ADMM. Figure 4 shows the mAP progress of YOLOv3-tiny during masked-retraining for 10 epochs, after pruned with 2× compression. SLR reaches its peak mAP only in the 3rd epoch, while ADMM can catch up to the same mAP after 10 epochs of retraining.

Table 3 shows the results of the 3D object detection model compression on the KITTI benchmark. The SLR/ADMM results are reported after 40 epochs of training and 3 epochs of masked-retraining. **We have 2 observations:** First, SLR has a much higher accuracy than ADMM after hardpruning with increased compression rate and “hard” strata as shown in Figure 3. For example, when tested under 9.44× compression, SLR mAP is more than 15% higher than ADMM as illustrated in Figure 3c. Also, in “easy” and “moderate” difficulty stratas, as shown in Figure 3a and Figure 3b, SLR hard-pruning mAP is still more than 10% higher than ADMM under 9.44× compression. Secondly, we observe that since SLR has higher mAP after hard-pruning, it also significantly higher mAP after retraining. There is almost 16% mAP difference between SLR and ADMM in the “hard” difficulty level and 9.44× compression case.

Lastly, Table 4 reports our result for the Lane Detection task on TuSimple lane detection benchmark after 40 epochs of training and 3 epochs of masked-retraining. We conducted experiments under 3 different compression rates. Similarly, it can be seen that SLR has better performance over ADMM as compression rate increases.

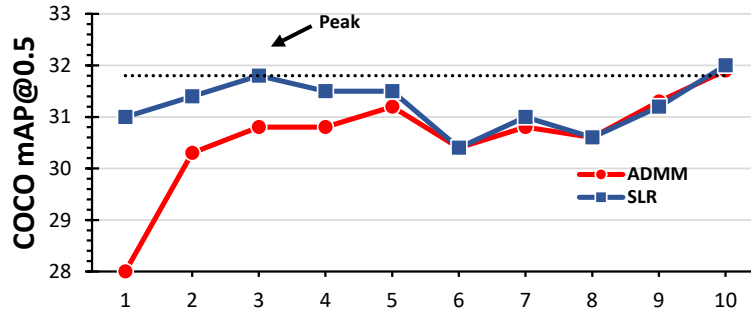


Figure 4: Retraining of YOLOv3-tiny on COCO benchmark for 10 epochs after pruning with SLR vs. ADMM.

#### 4.4 Ablation Studies

We conducted several experiments to observe SLR behavior with respect to SLR parameters  $\rho$ ,  $s_0$ ,  $r$  and  $M$  on ResNet-18 model (with 93.33% pretrained model accuracy) and CIFAR-10. We pruned the model through SLR training for 20 epochs with a compression rate of 1.96 and masked-retrained the hard-pruned model for 20 epochs. Table 5 shows the accuracy of the model based on the different values of  $s_0$  and  $\rho$ . Based on the accuracy after hard-pruning, it can be seen that  $s_0 = 10^{-4}$  and  $\rho = 0.1$  yield the best results. Figure 5 demonstrates that the

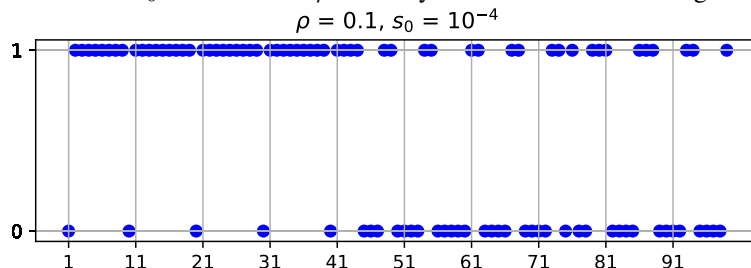


Figure 5: Surrogate optimality condition satisfaction graph during the SLR training of ResNet-18 on CIFAR-10 for 100 epochs (1: satisfied, 0: not satisfied). In the beginning of the training, condition is satisfied more frequently.

Table 5: ResNet-18 accuracy (%) on CIFAR-10 after SLR training, after hard pruning and after retraining with SLR in different  $\rho$ 's and initial step sizes.

$\rho$	$s_0$			
	0.01	0.001	0.0001	0.00001
0.1	86.89, <b>87.67</b> , 91.43	89.56, <b>89.80</b> , 91.43	90.46, <b>91.40</b> , 91.70	90.34, <b>91.24</b> , 92.03
0.01	89.97, <b>90.30</b> , 91.39	90.47, <b>90.74</b> , 91.69	90.28, <b>91.07</b> , 91.76	90.27, <b>90.83</b> , 91.99

surrogate optimality condition, the high-level convergence criterion of the SLR method, is satisfied periodically during training with  $s_0 = 10^{-4}$  and  $\rho = 0.1$ , thereby signifying that "good" multiplier-updating directions are always found.

Table 6 shows the results with respect to  $M = 100, 200, 300$  and  $r = 0.05, 0.1, 0.2$ , separately. Based on the accuracy after hard pruning,  $M = 200$  and  $r = 0.05$  give the best results. As a conclusion, we observe that parameters  $\rho = 0, 1, s_0 = 10^{-4}, r = 0.1$  and  $M = 200$  yield better performance for SLR.

Table 6: ResNet-18 performance on CIFAR-10 (accuracy after SLR training, after hard-pruning and after retraining) with different values of  $M$  and  $r$ .

<b>M</b>	<b>Accuracy (%)</b>	<b>r</b>	<b>Accuracy (%)</b>
100	90.46, <b>91.40</b> , 91.70	0.05	90.48, <b>91.38</b> , 92.22
200	91.09, <b>91.49</b> , 91.95	0.1	91.09, <b>91.49</b> , 91.95
300	90.01, <b>90.80</b> , 91.78	0.2	90.10, <b>90.61</b> , 91.73

## 5 Conclusions

In this paper, we presented the DNN weight-pruning problem as a non-convex optimization problem by adopting the cardinality function to induce sparsity of the weights. By using the Surrogate Lagrangian Relaxation (SLR) method, the relaxed weight-pruning problem is decomposed into subproblems. The subproblems are then efficiently coordinated by updating Lagrangian multipliers thereby resulting in fast convergence. We conducted weight-pruning experiments on image classification and object detection tasks to compare our SLR method against ADMM. We have observed that SLR has a significant advantage over ADMM under high compression rates and achieves better accuracy during weight pruning. SLR reduces the accuracy loss caused by the hard-pruning and subsequently reduces the long retraining process that is performed to recover from the accuracy loss. With the effective optimization capabilities through coordination with clear advantages shown from several examples, the SLR method has a strong potential for more general DNN-training applications.

## References

- [1] Alex Krizhevsky, Ilya Sutskever, and Geoffrey E Hinton. Imagenet classification with deep convolutional neural networks. In *Advances in neural information processing systems*, pages 1097–1105, 2012.
- [2] Karen Simonyan and Andrew Zisserman. Very deep convolutional networks for large-scale image recognition. *arXiv preprint arXiv:1409.1556*, 2014.
- [3] Song Han, Huizi Mao, and William J Dally. Deep compression: Compressing deep neural networks with pruning, trained quantization and huffman coding. *International Conference on Learning Representations (ICLR)*, 2016.
- [4] Song Han, Jeff Pool, John Tran, and William Dally. Learning both weights and connections for efficient neural network. In *Advances in Neural Information Processing Systems (NIPS)*, pages 1135–1143, 2015.
- [5] Xiaoliang Dai, Hongxu Yin, and Niraj K Jha. Nest: A neural network synthesis tool based on a grow-and-prune paradigm. *arXiv preprint arXiv:1711.02017*, 2017.
- [6] Tien-Ju Yang, Yu-Hsin Chen, and Vivienne Sze. Designing energy-efficient convolutional neural networks using energy-aware pruning. *arXiv preprint arXiv:1611.05128*, 2016.
- [7] Dmitry Molchanov, Arsenii Ashukha, and Dmitry Vetrov. Variational dropout sparsifies deep neural networks. In *International Conference on Machine Learning*, pages 2498–2507, 2017.

- [8] Yiwen Guo, Anbang Yao, and Yurong Chen. Dynamic network surgery for efficient dnns. In *Advances In Neural Information Processing Systems*, pages 1379–1387, 2016.
- [9] Frederick Tung, Srikanth Muralidharan, and Greg Mori. Fine-pruning: Joint fine-tuning and compression of a convolutional network with bayesian optimization. *arXiv preprint arXiv:1707.09102*, 2017.
- [10] Jian-Hao Luo, Jianxin Wu, and Weiyao Lin. Thinet: A filter level pruning method for deep neural network compression. In *2017 IEEE International Conference on Computer Vision (ICCV)*, pages 5068–5076. IEEE, 2017.
- [11] Wei Wen, Chunpeng Wu, Yandan Wang, Yiran Chen, and Hai Li. Learning structured sparsity in deep neural networks. In *Advances in Neural Information Processing Systems*, pages 2074–2082, 2016.
- [12] Baoyuan Liu, Min Wang, Hassan Foroosh, Marshall Tappen, and Marianna Pensky. Sparse convolutional neural networks. In *Proceedings of the IEEE Conference on Computer Vision and Pattern Recognition*, pages 806–814, 2015.
- [13] Hao Zhou, Jose M Alvarez, and Fatih Porikli. Less is more: Towards compact cnns. In *European Conference on Computer Vision*, pages 662–677. Springer, 2016.
- [14] Wenlin Chen, James Wilson, Stephen Tyree, Kilian Weinberger, and Yixin Chen. Compressing neural networks with the hashing trick. In *International Conference on Machine Learning*, pages 2285–2294, 2015.
- [15] Eunhyeok Park, Junwhan Ahn, and Sungjoo Yoo. Weighted-entropy-based quantization for deep neural networks. In *IEEE Conference on Computer Vision and Pattern Recognition (CVPR)*, 2017.
- [16] Hao Li, Asim Kadav, Igor Durdanovic, Hanan Samet, and Hans Peter Graf. Pruning filters for efficient convnets. *arXiv preprint arXiv:1608.08710*, 2016.
- [17] Jonathan Frankle and Michael Carbin. The lottery ticket hypothesis: Finding sparse, trainable neural networks. *arXiv preprint arXiv:1803.03635*, 2018.
- [18] Zhuang Liu, Mingjie Sun, Tinghui Zhou, Gao Huang, and Trevor Darrell. Rethinking the value of network pruning. In *International Conference on Learning Representations*, 2019.
- [19] Tianyun Zhang, Shaokai Ye, Kaiqi Zhang, Jian Tang, Wujie Wen, Makan Fardad, and Yanzhi Wang. A systematic dnn weight pruning framework using alternating direction method of multipliers. In *Proceedings of the European Conference on Computer Vision (ECCV)*, pages 184–199, 2018.
- [20] Mikhail A. Bragin, Peter B. Luh, Joseph H. Yan, Nanpeng Yu, and Gary A. Stern. Convergence of the surrogate lagrangian relaxation method. *Journal of Optimization Theory and Applications*, 164(1):173–201, 2015.
- [21] Song Han, Jeff Pool, John Tran, and William Dally. Learning both weights and connections for efficient neural network. In *Advances in neural information processing systems*, pages 1135–1143, 2015.
- [22] Yihui He, Xiangyu Zhang, and Jian Sun. Channel pruning for accelerating very deep neural networks. In *Computer Vision (ICCV), 2017 IEEE International Conference on*, pages 1398–1406. IEEE, 2017.
- [23] Stephen Boyd, Neal Parikh, and Eric Chu. *Distributed optimization and statistical learning via the alternating direction method of multipliers*. Now Publishers Inc, 2011.
- [24] Wei Niu, Xiaolong Ma, Sheng Lin, Shihao Wang, Xuehai Qian, Xue Lin, Yanzhi Wang, and Bin Ren. Patdnn: Achieving real-time dnn execution on mobile devices with pattern-based weight pruning. In *Proceedings of the Twenty-Fifth International Conference on Architectural Support for Programming Languages and Operating Systems*, pages 907–922, 2020.
- [25] Zhengang Li, Yifan Gong, Xiaolong Ma, Sijia Liu, Mengshu Sun, Zheng Zhan, Zhenglun Kong, Geng Yuan, and Yanzhi Wang. Ss-auto: A single-shot, automatic structured weight pruning framework of dnns with ultra-high efficiency. *arXiv preprint arXiv:2001.08839*, 2020.
- [26] Stephen Boyd, Neal Parikh, Eric Chu, Borja Peleato, and Jonathan Eckstein. Distributed optimization and statistical learning via the alternating direction method of multipliers. *Foundations and Trends® in Machine Learning*, 3(1):1–122, 2011.
- [27] M. A. Bragin, P. B. Luh, B. Yan, and X. Sun. A scalable solution methodology for mixed-integer linear programming problems arising in automation. *IEEE Transactions on Automation Science and Engineering*, 16(2):531–541, 2019.
- [28] X. Zhao, P. B. Luh, and J. Wang. Surrogate gradient algorithm for lagrangian relaxation. *Journal of Optimization Theory and Applications*, 100:699–712, 1999.
- [29] Kaiming He, Xiangyu Zhang, Shaoqing Ren, and Jian Sun. Deep residual learning for image recognition. In *Proceedings of the IEEE Conference on Computer Vision and Pattern Recognition*, pages 770–778, 2016.
- [30] Andreas Geiger, Philip Lenz, and Raquel Urtasun. Are we ready for autonomous driving? the kitti vision benchmark suite. In *2012 IEEE Conference on Computer Vision and Pattern Recognition*, pages 3354–3361. IEEE, 2012.
- [31] Joseph Redmon and Ali Farhadi. Yolov3: An incremental improvement. *CoRR*, abs/1804.02767, 2018.
- [32] Alex H Lang, Sourabh Vora, Holger Caesar, Lubing Zhou, Jiong Yang, and Oscar Beijbom. Pointpillars: Fast encoders for object detection from point clouds. In *Proceedings of the IEEE Conference on Computer Vision and Pattern Recognition*, pages 12697–12705, 2019.
- [33] Zequn Qin, Huanyu Wang, and Xi Li. Ultra fast structure-aware deep lane detection. *arXiv preprint arXiv:2004.11757*, 2020.

## A Supplementary Experimental Results

### A.1 Surrogate Optimality Condition

Figure 6 shows the surrogate optimality condition after each epoch of SLR training of ResNet-18 on CIFAR-10 dataset with different  $\rho$  and  $s_0$  values. It can be seen that surrogate optimality condition is satisfied more frequently with a selection of smaller step sizes as compared to larger ones.

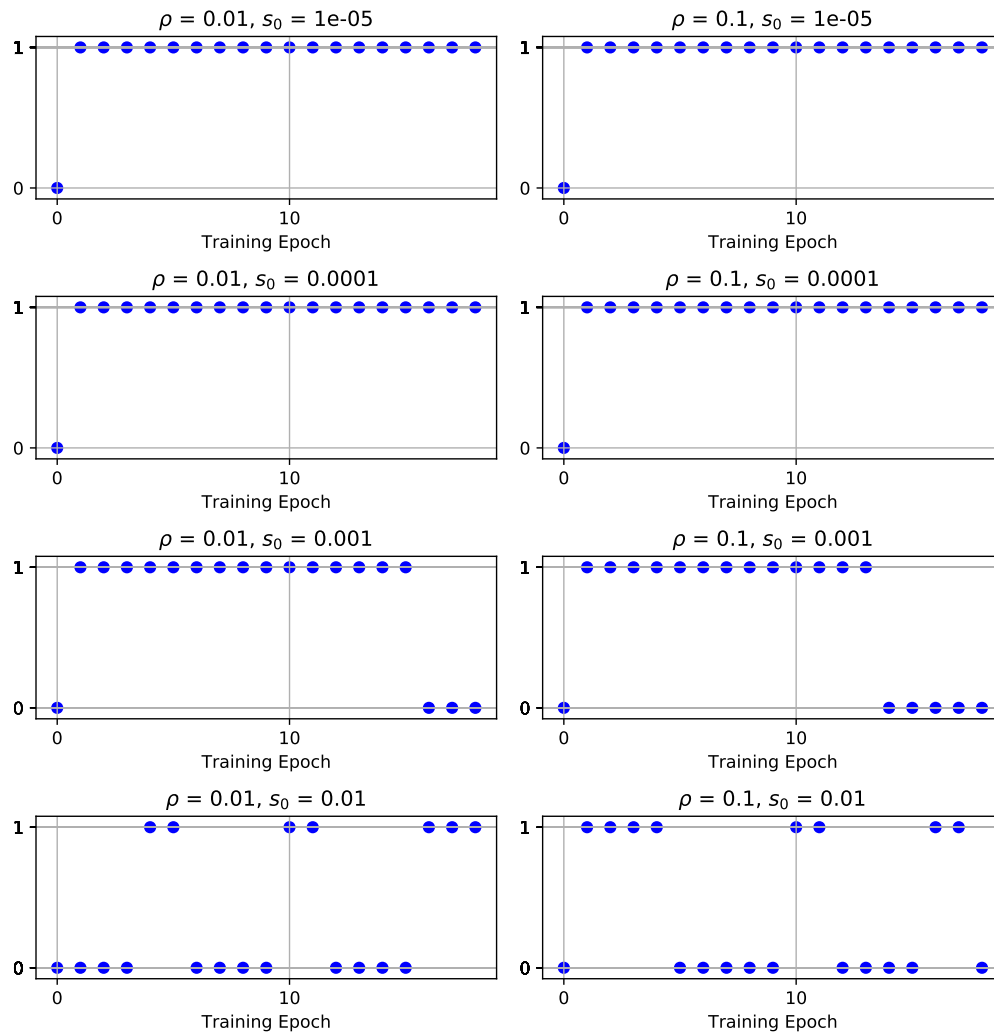


Figure 6: Surrogate optimality condition during the SLR training of ResNet-18 with different values  $\rho$  and stepsize  $s_0$  (1: satisfied, 0: not satisfied).

As a following experiment, we compare the retraining accuracy of the models pruned with small and large step sizes. Figure 7 shows the accuracy curves. They start off with a gap between their accuracy. The model with the low initial accuracy ( $s_0 = 0.01$ ) takes longer to reach the accuracy of the pruned model with higher initial accuracy. Moreover, the model with higher initial accuracy ( $s_0 = 10^{-5}$ ) achieves a higher peak accuracy during the 20-epoch retraining phase. That demonstrates the importance of accuracy after hard-pruning.

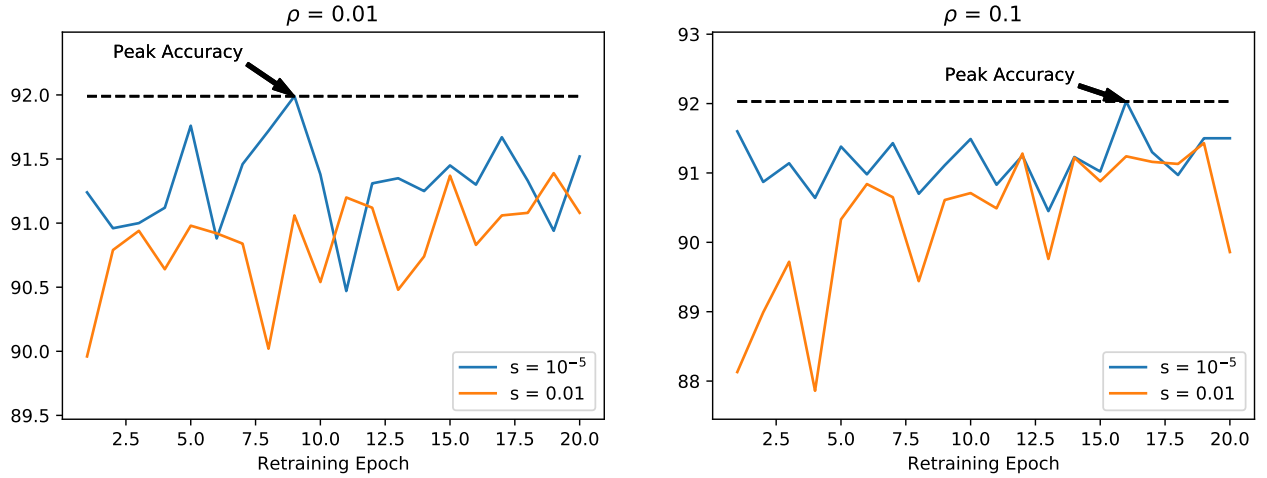


Figure 7: Retraining accuracy of the pruned models with the small and large step sizes on ResNet-18.

## A.2 Comparison of SLR and ADMM Training

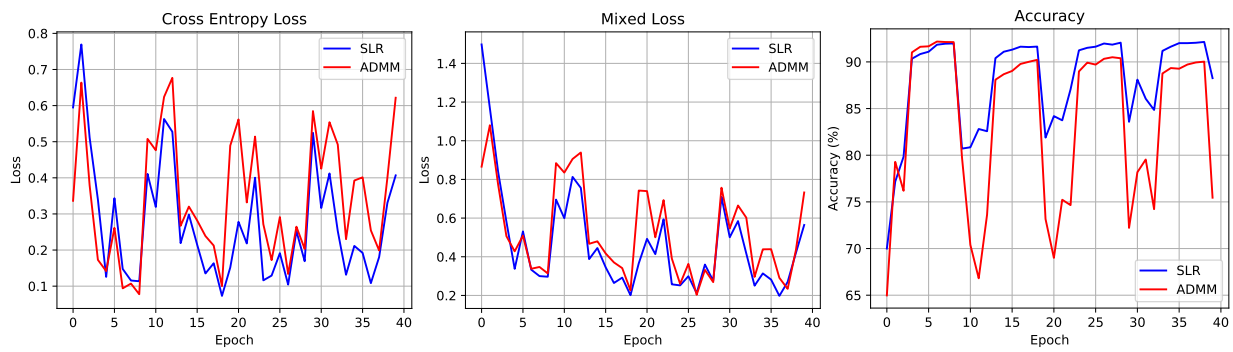
Table 7 and 8 show the comparison of ADMM and SLR on CIFAR-10 and ImageNet benchmarks with different compression rates, respectively. In these experiments, we set the SLR parameters as  $\rho = 0.1$ ,  $s_0 = 10^{-4}$ ,  $M = 200$ ,  $r = 0.1$ . In CIFAR-10 experiments, we used a learning rate of 0.01, batch size of 128 and ADAM optimizer during training. On ImageNet, we used a learning rate of  $10^{-4}$ , batch size of 256 and SGD optimizer. CIFAR-10 results report the retraining accuracy only after 5 epochs, and ImageNet results show the accuracy after 3 epochs of retraining.

Table 7: Comparison of SLR and ADMM on CIFAR-10 - ResNet-18.

Compression Rate	Optimization	After Training (%)	After Hardpruning (%)	After Retraining (%)
1.96×	SLR	88.34	<b>89.28</b>	90.46
	ADMM	90.08	90.86	90.58
3.21×	SLR	89.15	<b>91.03</b>	91.27
	ADMM	85.85	89.32	90.3
4.69×	SLR	89.31	<b>90.13</b>	90.5
	ADMM	86.88	88.7	90.47
6.09×	SLR	88.14	<b>88.68</b>	91.19
	ADMM	79.5	84.22	90.57
8.71×	SLR	88.26	<b>88.12</b>	90.37
	ADMM	75.45	80.25	89.73

Table 8: Comparison of SLR and ADMM on ImageNet - ResNet-18.

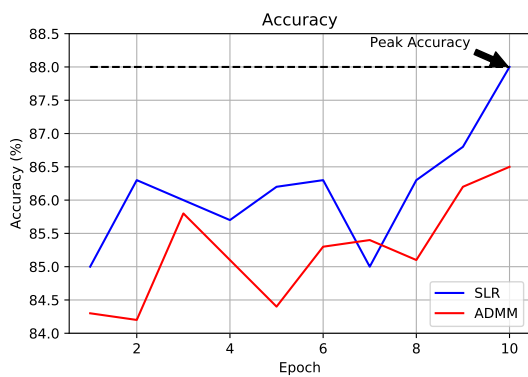
Compression Rate	Optimization	After Training (%)	After Hardpruning (%)	After Retraining (%)
4.03 $\times$	ADMM	85.98	86.07	87.53
	SLR	86.65	<b>86.21</b>	87.69
6.50 $\times$	ADMM	81.37	80.69	85.23
	SLR	83.00	<b>83.31</b>	85.66
7.15 $\times$	ADMM	81.29	80.66	85.11
	SLR	82.76	<b>83.14</b>	85.37



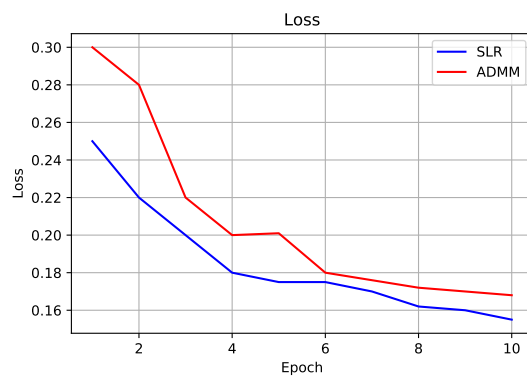
(a) Cross entropy loss during training.

(b) Mixed loss during training.

(c) Training Accuracy.



(d) Retraining Accuracy.



(e) Retraining Loss.

Figure 8: Comparison of SLR and ADMM on ResNet-18 - CIFAR-10 with 8.71 $\times$  compression.

Figure 8 ~ 11 show the detailed results with ADMM and SLR training and retraining from our experiments. The heatmaps of model weights for 5 layers before pruning, after SLR training and after hardpruning are shown in Section A.3. Additionally, the heatmaps of model weights after SLR and ADMM training are compared in Section A.4.

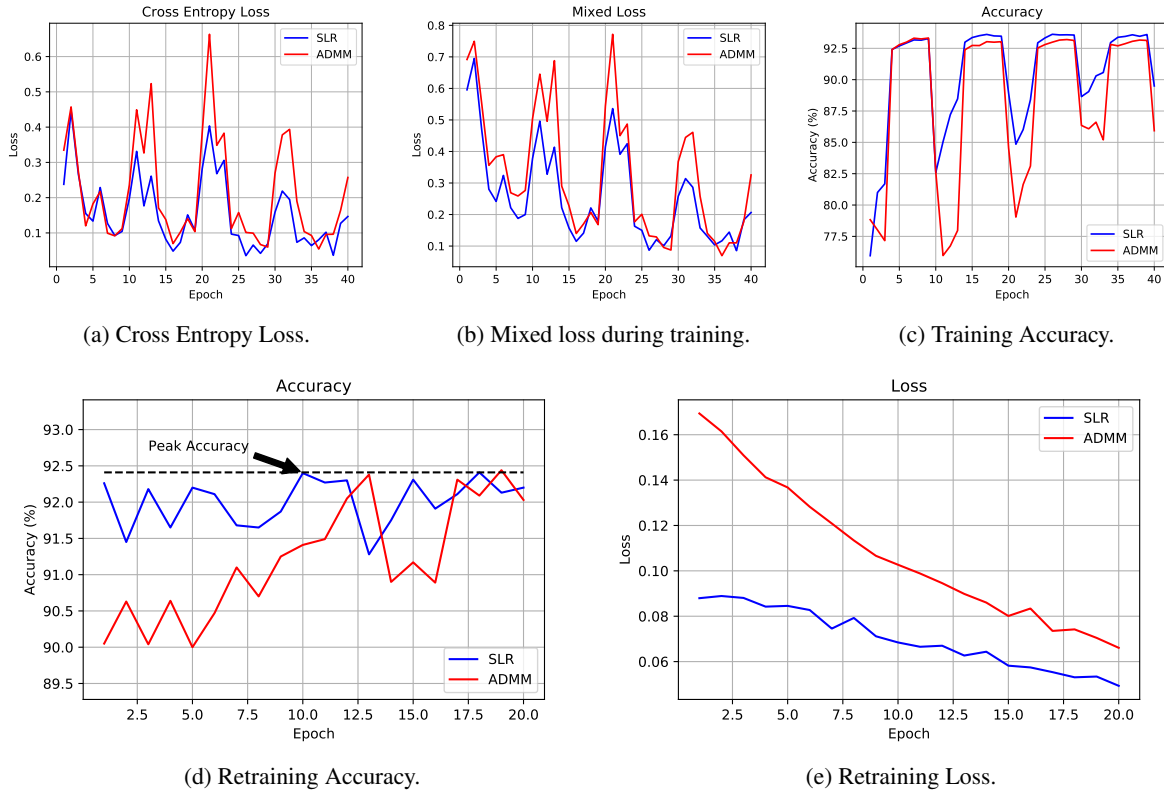
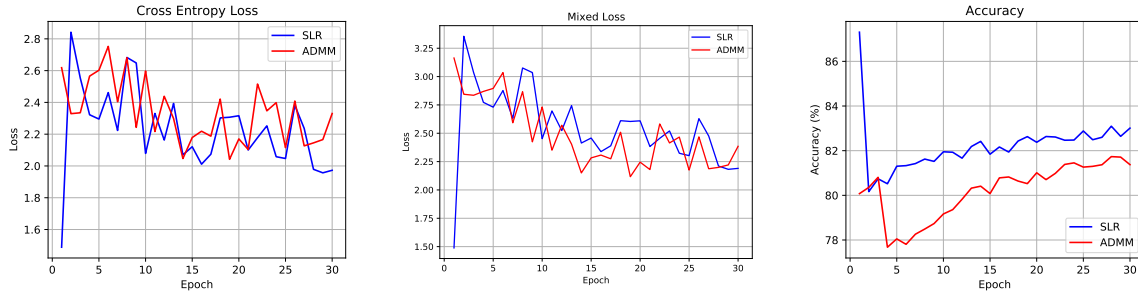


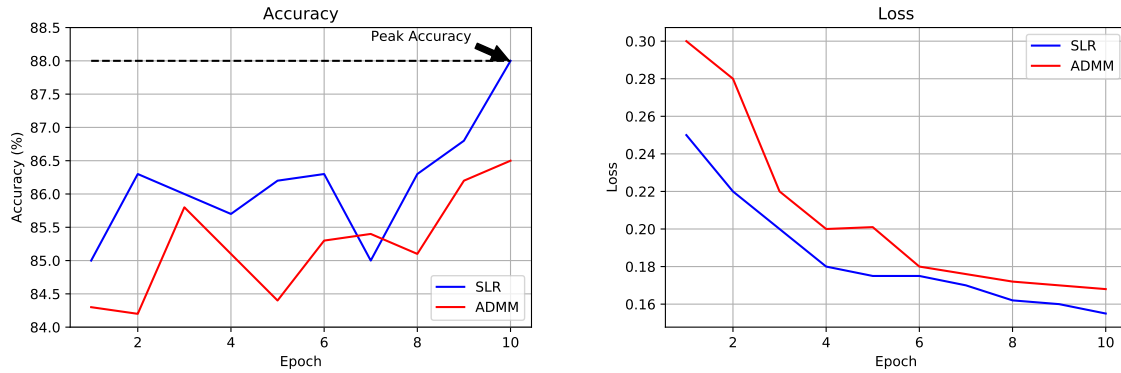
Figure 9: Comparison of SLR and ADMM on ResNet-50 - CIFAR-10 with  $3.4\times$  compression.

In Figure 8 and Figure 9, our comparison of SLR and ADMM on CIFAR-10 benchmark can be seen, for ResNet-18 and ResNet-50 respectively. Overall, for both experiments, we observe that ADMM loss and accuracy during training are less stable than SLR. Therefore, during retraining, the model pruned with SLR has an advantage of a higher accuracy and less cross entropy loss as compared to the one with ADMM. Thus, SLR’s peak accuracy after in 10 epochs of retraining remains higher than ADMM.

Figure 10 and Figure 11 show our comparison of SLR and ADMM on ImageNet benchmark for ResNet-18 and ResNet-50 respectively. During training, ADMM experiences a higher loss in accuracy compared to SLR. Therefore, the models pruned with SLR can recover their accuracy faster than ADMM during retraining. In both experiments, we observe the retraining accuracy for 10 epochs and observe that ADMM cannot reach the peak accuracy of SLR.

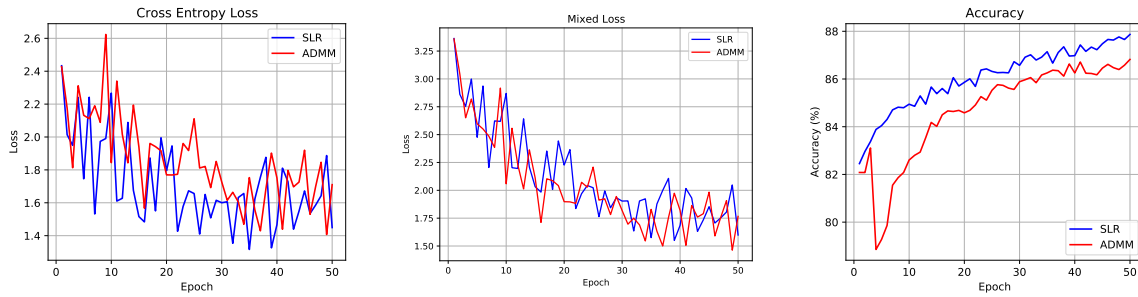


(a) Cross entropy loss during training. (b) Mixed loss during training. (c) Training Accuracy.

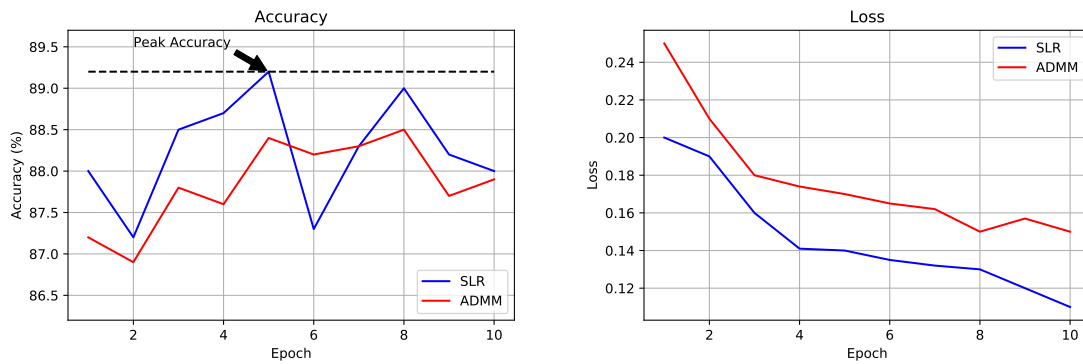


(d) Retraining Accuracy. (e) Retraining Loss.

Figure 10: Comparison of SLR and ADMM on ResNet-18 - ImageNet with  $6.5\times$  compression.



(a) Cross entropy loss during training. (b) Mixed loss during training. (c) Training Accuracy.



(d) Retraining Accuracy. (e) Retraining Loss.

Figure 11: Comparison of SLR and ADMM on ResNet-50 - ImageNet with  $3.89\times$  compression.

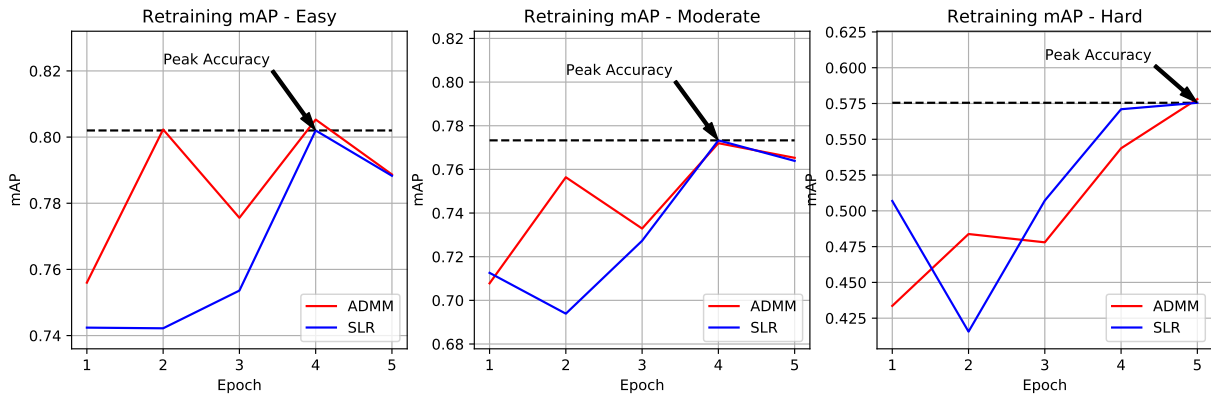


Figure 12: Retraining mAP of PointPillars model on KITTI benchmark in different task difficulty levels after pruned with  $9.44\times$  compression.

### A.3 Heatmaps for SLR-based Weight Pruning

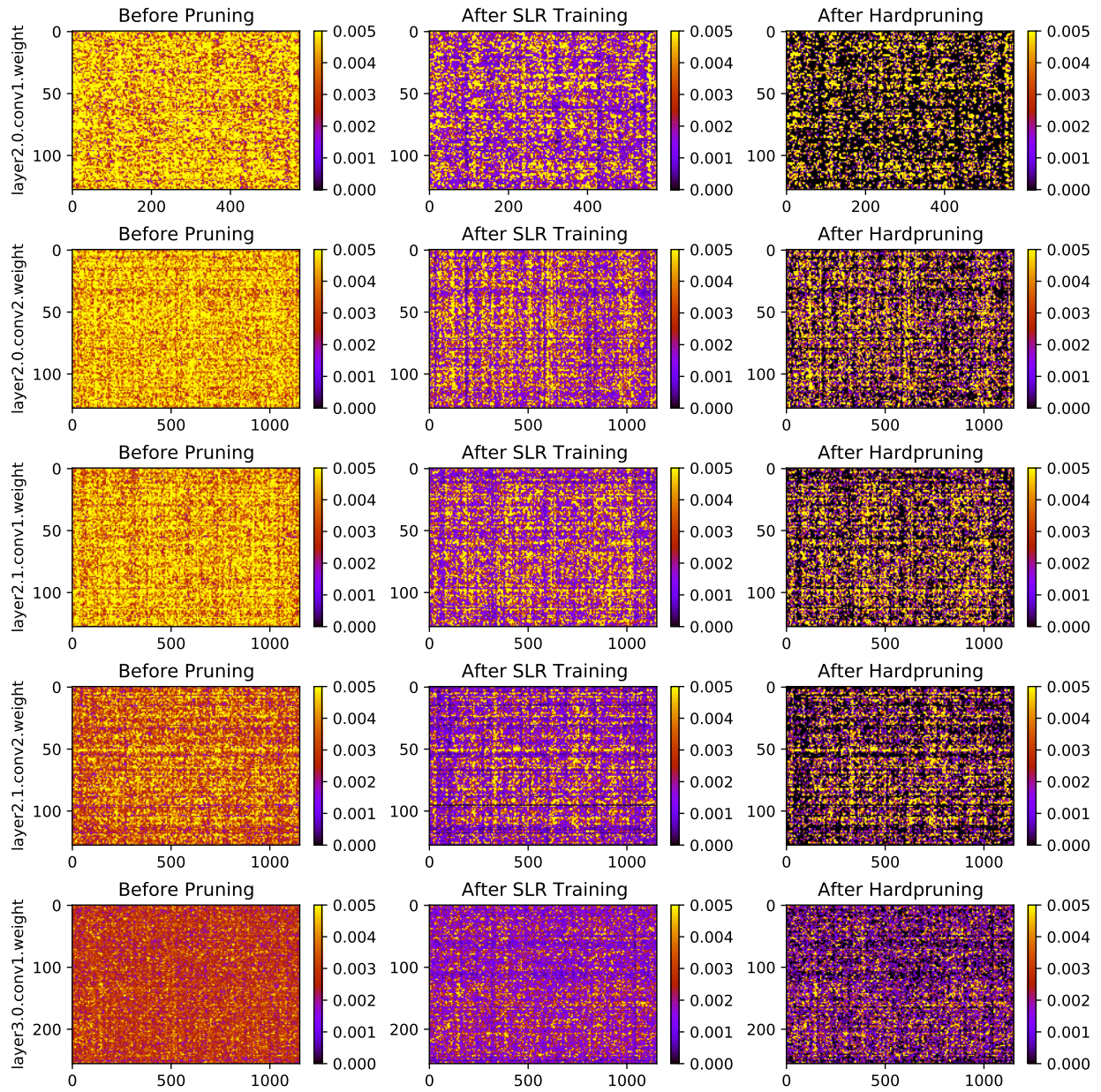


Figure 13: Heatmap of ResNet-18 weights after pruning with SLR on CIFAR-10.

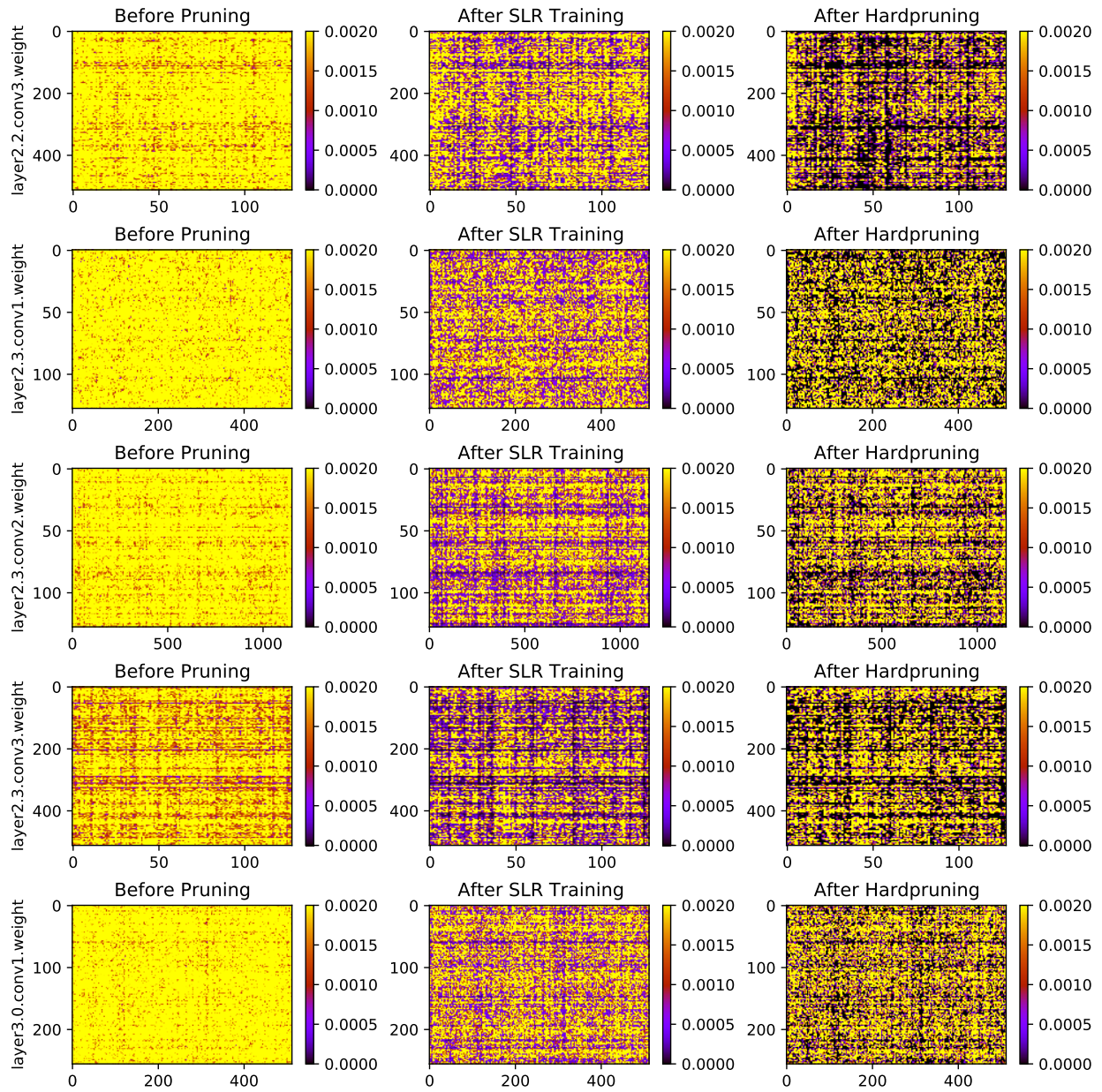


Figure 14: Heatmap of ResNet-50 weights after pruning with SLR on CIFAR-10.

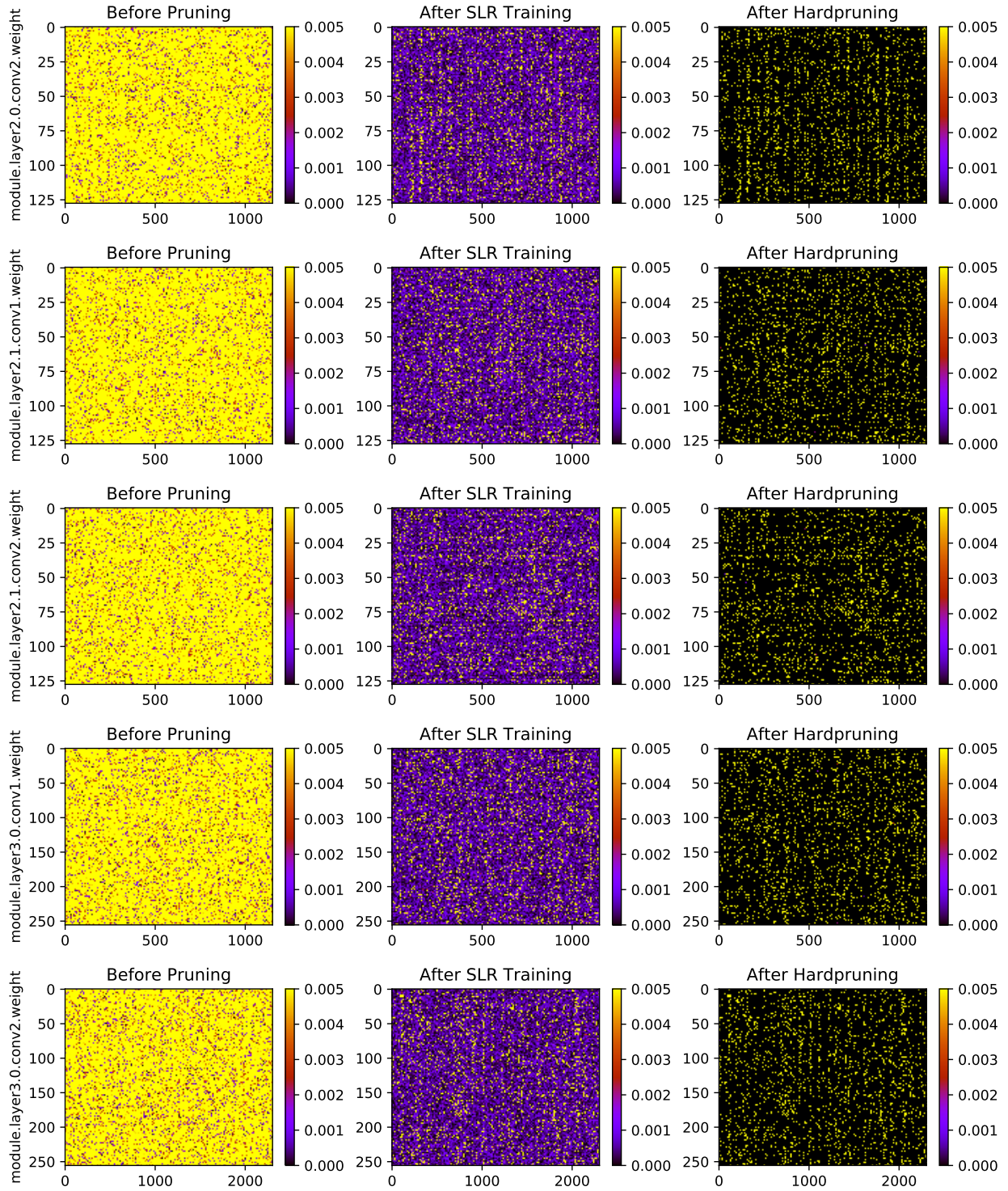


Figure 15: Heatmap of ResNet-18 weights after pruning with SLR on ImageNet.

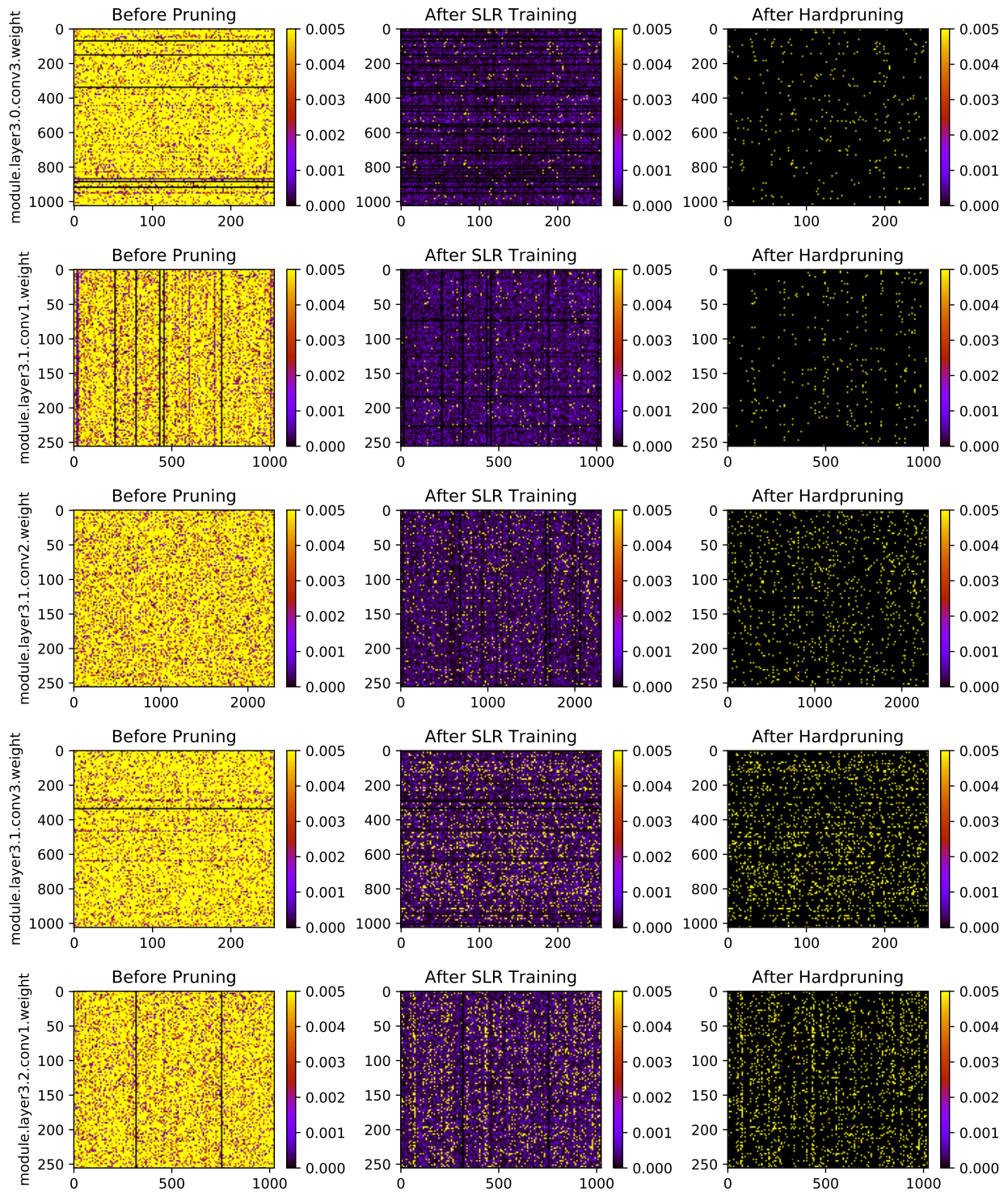


Figure 16: Heatmap of ResNet-50 weights after pruning with SLR on ImageNet.

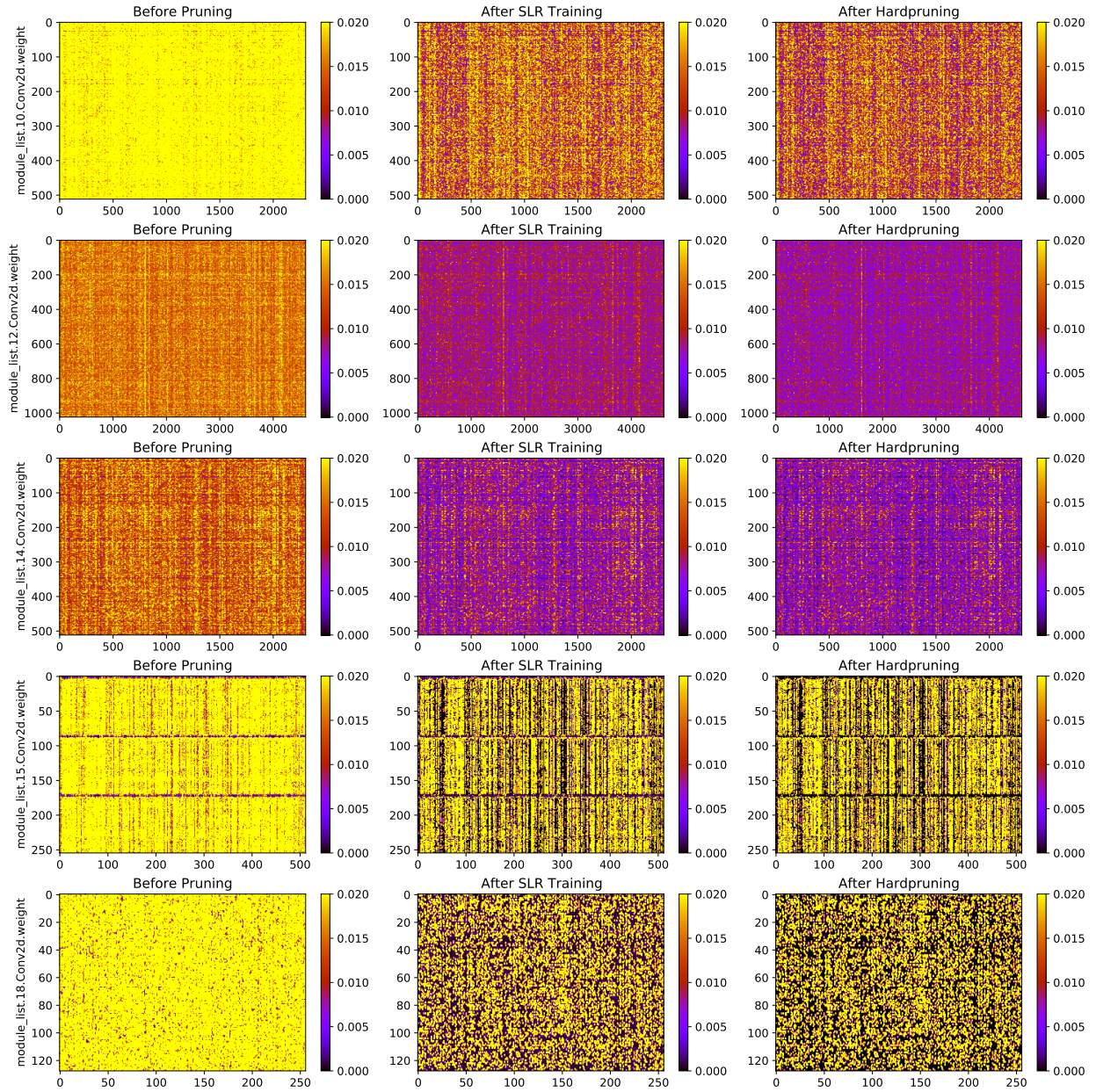


Figure 17: Heatmap of YOLOv3-tiny weights after pruning with SLR on COCO benchmark.

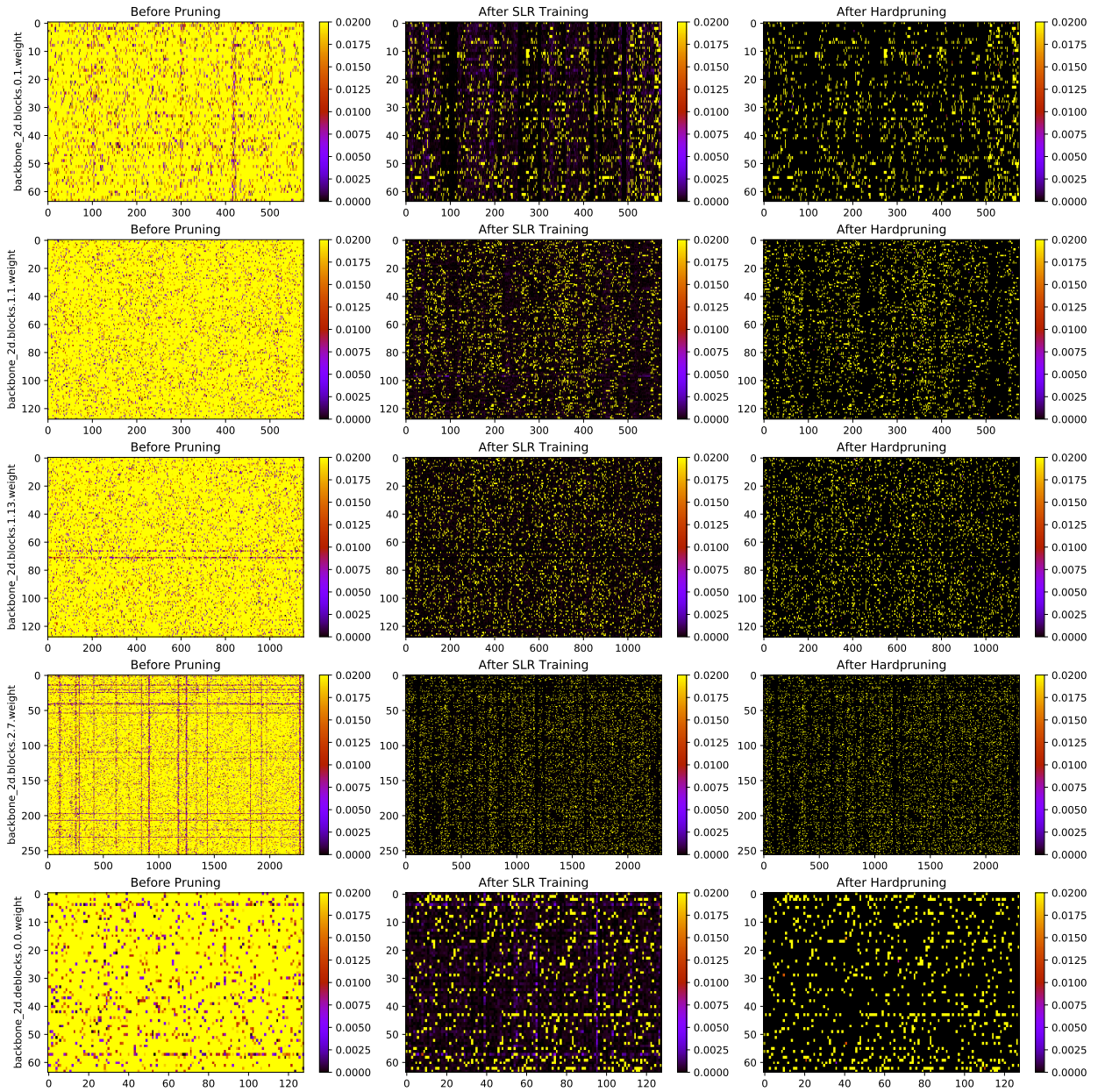


Figure 18: Heatmap of PointPillars weights after pruning with SLR on KITTI benchmark.

#### A.4 Heatmaps for SLR and ADMM Comparison

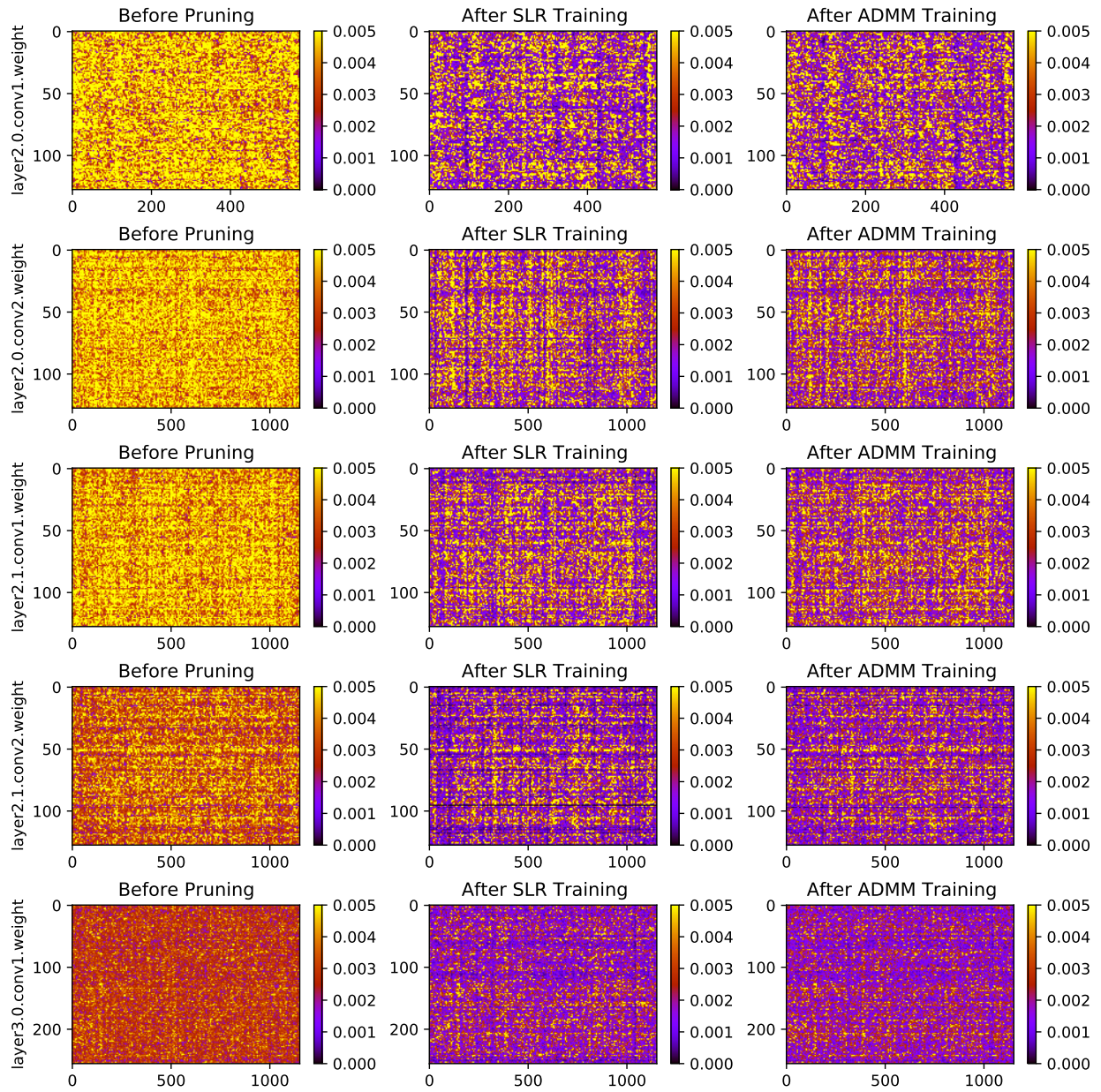


Figure 19: Heatmap of ResNet-18 weights after pruning with SLR and ADMM on CIFAR-10.

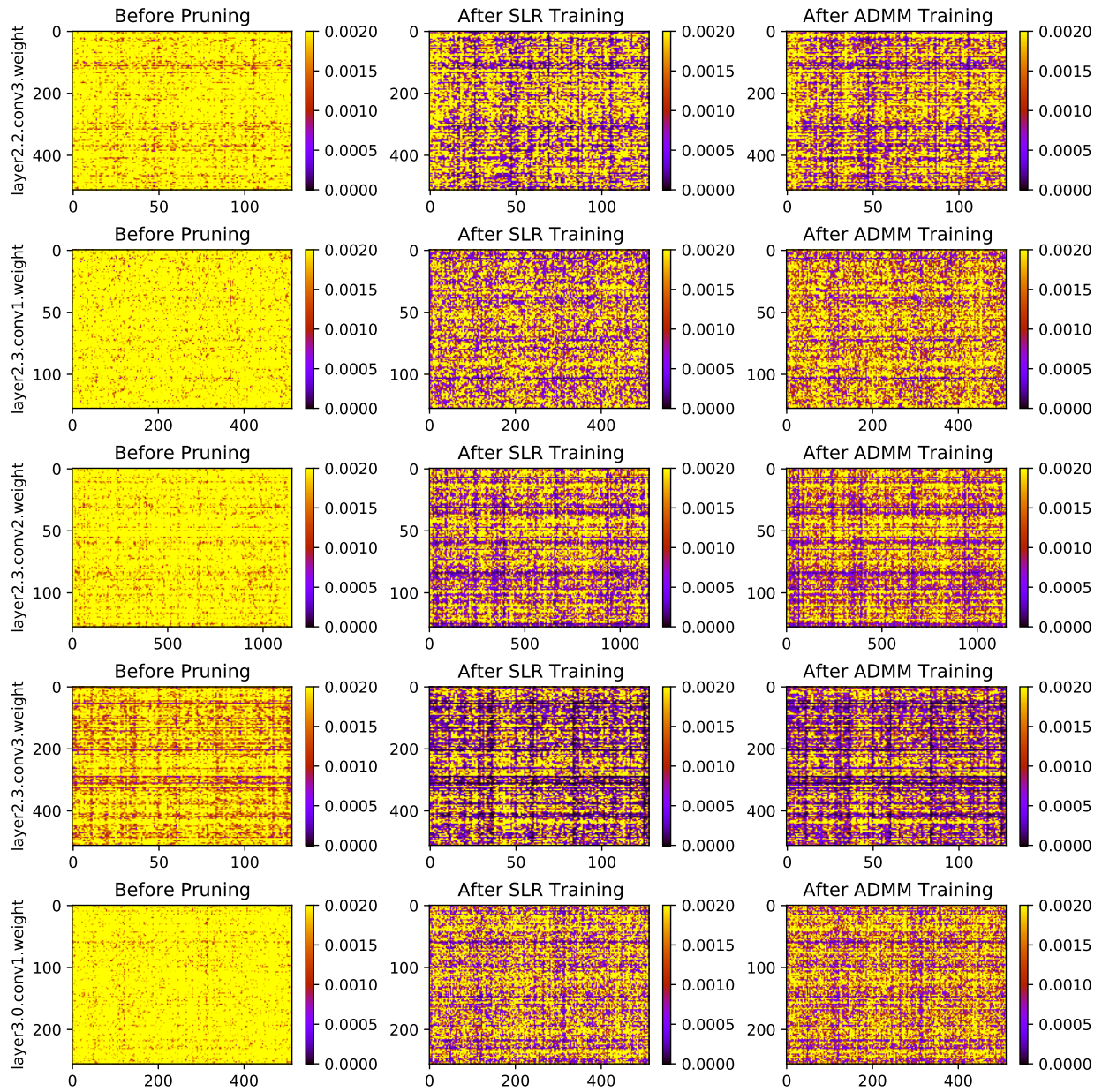


Figure 20: Heatmap of ResNet-50 weights after pruning with SLR and ADMM on CIFAR-10.

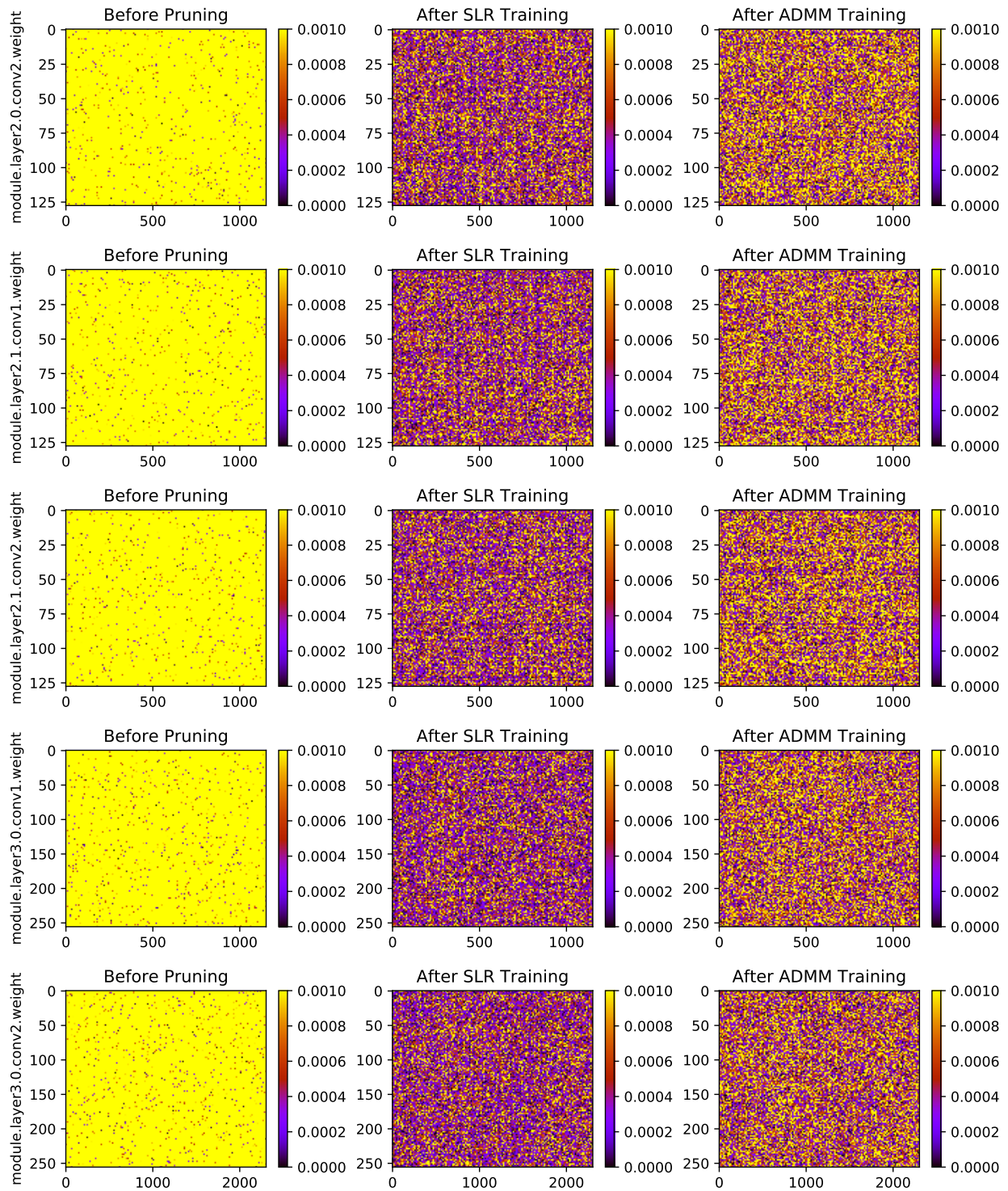


Figure 21: Heatmap of ResNet-18 weights after pruning with SLR and ADMM on ImageNet.

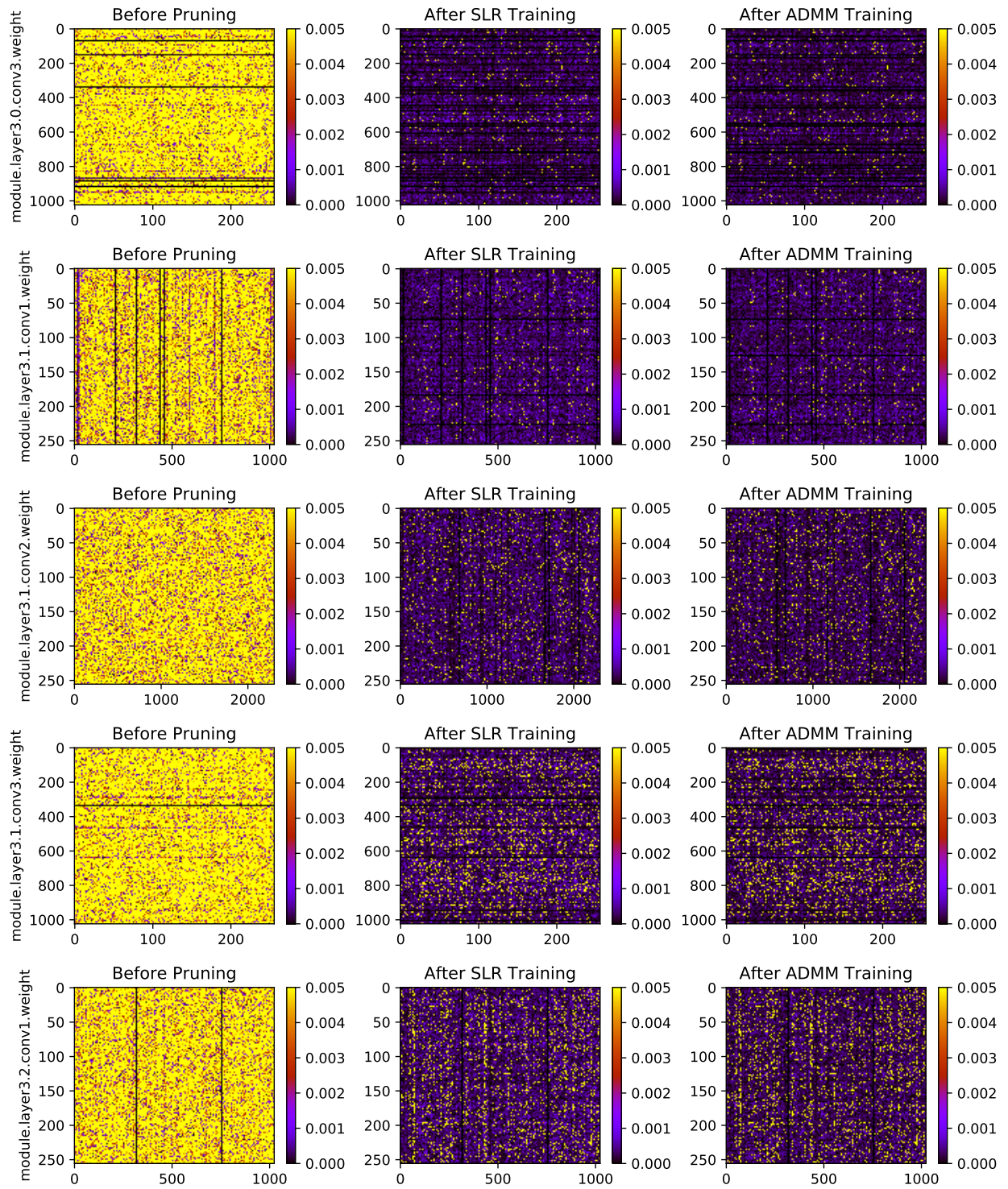


Figure 22: Heatmap of ResNet-50 weights after pruning with SLR and ADMM on ImageNet.

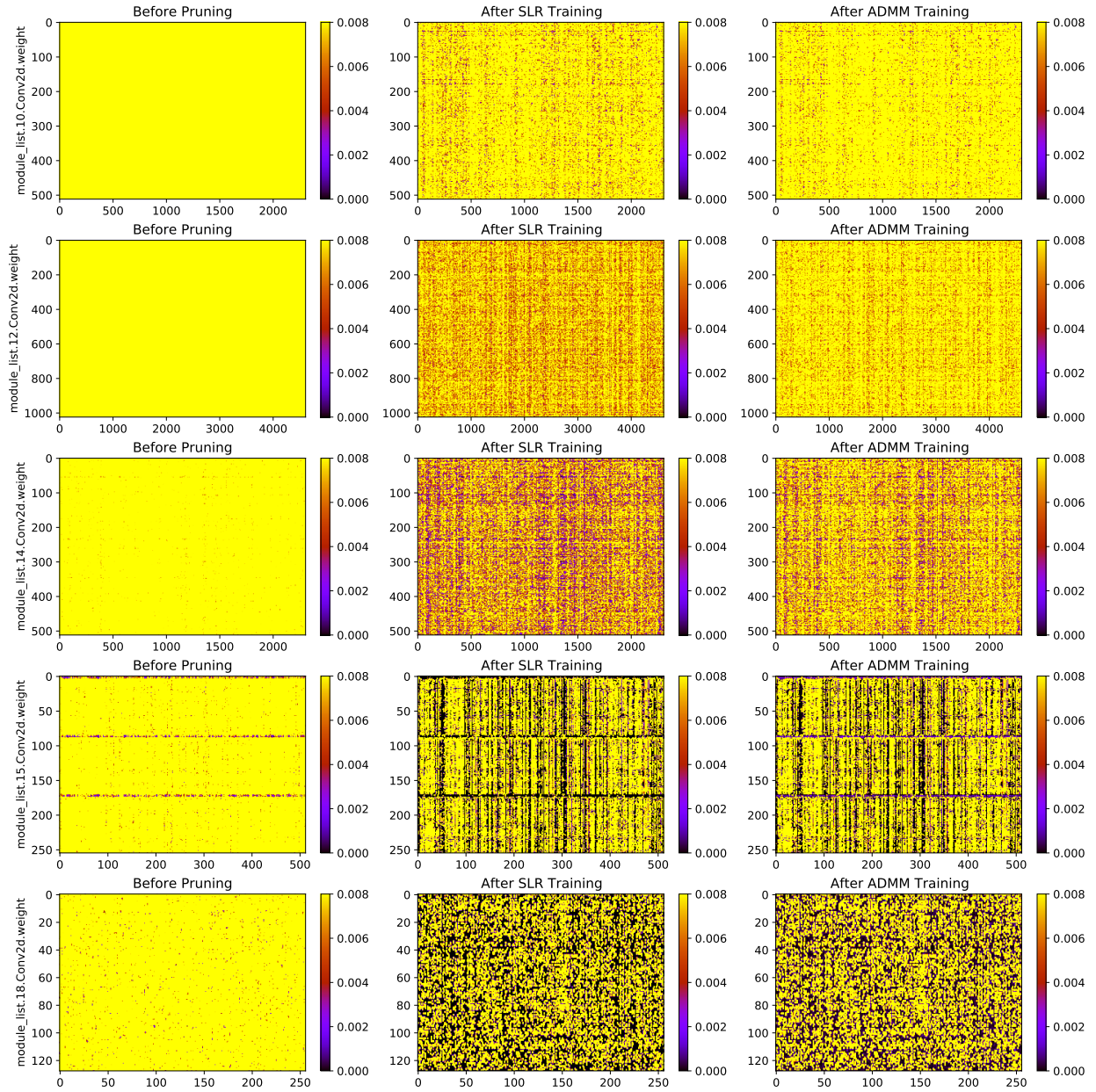


Figure 23: Heatmap of YOLOv3-tiny weights after pruning with SLR and ADMM on COCO benchmark.

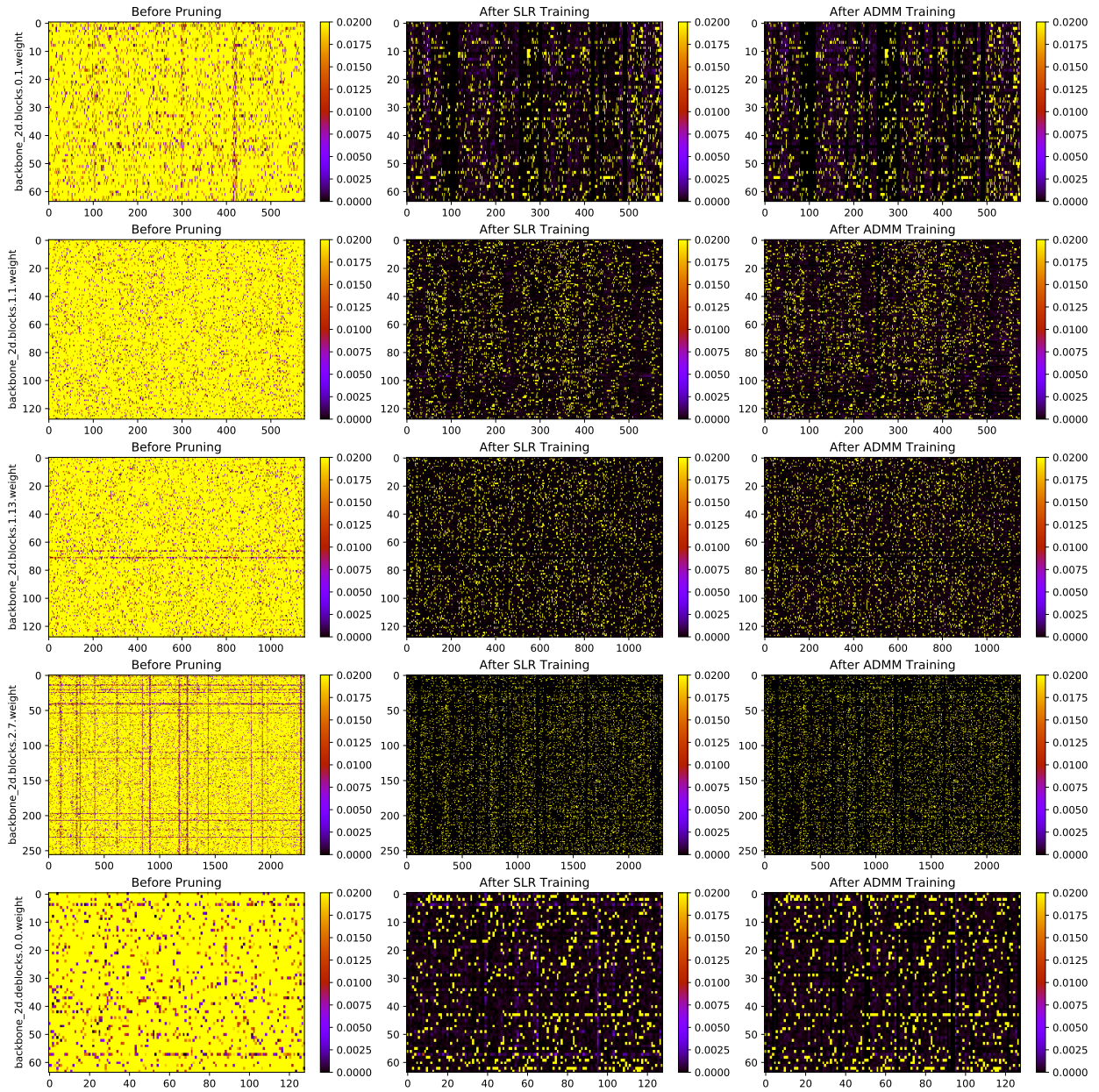


Figure 24: Heatmap of PointPillars weights after pruning with SLR and ADMM on KITTI benchmark.